JAERI-M
82-124

BLOWDOWN FORCE ANALYSIS OF PIPING SYSTEM UNDER LOCA CONDITIONS USING BLOWDOWN CODE

September 1982

Noriyuki MIYAZAKI and Takashi AKIMOTO*

日本原子力研究所
Japan Atomic Energy Research Institute

JAERI-M レポートは，日本原子力研究所が不定期に公刊している研究報告書です。
入手の問合わせは，日本原子力研究所技術情報部情報資料課（〒319－11 茨城県那珂郡東海村）あて，お申しこしください。なお，このほかに財団法人原子力弘済会資料センター（〒319-11 茨城県那珂郡東海村日本原子力研究所内）で複写による実費頒布をおこなっております。

JAERI-M reports are issued irregularly.
Inquiries about availability of the reports should be addressed to Information Section, Division of Technical Information, Japan Atomic Energy Research Institute, Tokai-mura, Naka-gun, Ibaraki-ken 319-11, Japan.

編集兼発行　日本原子力研究所
印　　刷　山田軽印刷所

JAERI-M 82-124

Blowdown Force Analysis of Piping System under LOCA Conditions Using BLOWDOWN Code

Noriyuki MIYAZAKI and Takashi AKIMOTO*

Division of Nuclear Safety Research
Tokai Research Establishment, JAERI

(Received August 12, 1982)

The BLOWDOWN code was developed for the blowdown force analysis of the piping system under the LOCA conditions. This is a post-processor of the thermal-hydraulic analysis code RELAP4/MOD6. The results obtained from the RELAP4/MOD6 code are converted into the blowdown forces by the BLOWDOWN code.

In the paper is described the outline of the BLOWDOWN code. Some numerical examples are also presented to show the effectiveness and limitation of the code.

Keywords: BLOWDOWN Code, Blowdown Force, Post Processor, Thermal-Hydraulic Analysis, RELAP4/MOD6, LOCA Conditions, Piping System

---

This work was performed under the contract between the Science and Technology Agency of Japan and JAERI to demonstrate the safety for pipe rupture of the primary coolant circuit in nuclear power plants.

* Century Research Center Corpotation

JAERI－M 82－124

LOCA時に配管系に作用するブローダウン力の BLOWDOWNコードによる解析

日本原子力研究所東海研究所安全工学部
宮崎　則幸・秋本　敬史*

（1982年8月12日受理）

LOCA時に配管系に作用するブローダウン力を解析するためにBLOWDOWNコードを開発した。このコードは熱流体解析コードRELAP4/MOD6のポストプロセッサである。すなわち，BLOWDOWNコードではRELAP4/MOD6コードの結果をブローダウン力に変換する。

本報ではBLOWDOWNコードの概略を述べるとともに，いくつかの解析例により本コードの有効性及び限界を明らかにした。

この報告書は，電源開発促進対策特別会計施行令に基づき，科学技術庁から日本原子力研究所への委託研究，昭和55年度配管信頼性実証試験のうち，ブローダウン力解析コードBLOWDOWNの概要および解析結果についてまとめたものである。

＊センチュリリサーチセンター㈱

CONTENTS

目　　次

1. Introduction

The loss-of-coolant accident, LOCA, must be taken into account in designing nuclear power plants. This accident is assumed to be triggered by an instantaneous pipe rupture. The dynamic motion of the pipe called pipe whip will be caused by the blowdown force acting on the ruptured pipe, if an instantaneous pipe rupture occurs. In LWR nuclear power plants, pipe whip restraints are installed to limit the movement of the whipping pipe and to protect such surrounding structures as the piping and containment against pipe whipping. In designing the piping of nuclear power plants, the pipe whip analysis of the pipe-restraint system is implemented by using a finite element structural analysis code. The time history of the blowdown force is required in such an analysis.

The RELAP4/MOD6 code[1] is widely used to analyze the thermal-hydraulic transients under the LOCA conditions. This code provides all the quantities required for calculating the blowdown force.
The BLOWDOWN code, a post-processor of the RELAP4/MOD6 code, was developed for the blowdown force analysis of the piping system under the LOCA conditions. The PRTHRUST-J1 code[2](*) and the REPIPE code[3] have been already developed for the calculation of the blowdown force.
The PRTHRUST-J1 code is based on the RELAP3 code for the thermal-hydraulic analysis and uses the method proposed by Strong and Bahiere[4] to calculate the blowdown force. On the other hand, the REPIPE code is a post-processor of the RELAP4 code and uses the method proposed by Moody[5] for the calculation of the blowdown force. The blowdown force at a bend pipe is, however, not exactly dealt with in these codes. Namely, the fluid force due to the momentum change at the bend pipe is not taken into consideration. Therefore, the exact formulation is given in the BLOWDOWN code to calculate the blowdown force at the bend pipe.

In order to show the effectiveness and limitation of the code, several numerical analyses were performed by the BLOWDOWN code and those results were compared with those of other analyses or the experiments.

(*) The PRTHRUST-J1 code is a modified version of the PRTHRUST 1.0 code developed by Quadrex Corporation

2. Theoretical Background of the BLOWDOWN Code

The basic equation is the following Navier-Stokes equation.

$$\rho\left\{\frac{\partial \mathbf{u}}{\partial t} + (\mathbf{u}\cdot\mathrm{grad})\mathbf{u}\right\} = \rho\mathbf{g} - \mathrm{grad}(p) + \mu\{\nabla^2\mathbf{u} + \mathrm{grad}(\mathrm{div}\mathbf{u})\} - \lambda\,\mathrm{grad}(\mathrm{div}\mathbf{u}) \tag{1}$$

The following equation can be obtained by integrating eq.(1) over a control volume V, together with using the equation of continuity and the Gauss' divergence theorem.

$$\frac{\partial}{\partial t}\int_V \rho\mathbf{u}\,dV + \int_S \rho\mathbf{u}(\mathbf{u}\cdot\mathbf{n})dS = -\int_S p\mathbf{n}dS - \int_S \boldsymbol{\tau}dS + \mathbf{g}\int_V \rho dV \tag{2}$$

Now, let us consider a control volume as shown in Fig.1, where the surface S is divided into three parts S_1, S_2 and S_3. Considering that the product of the vectors $\mathbf{u}$ and $\mathbf{n}$ is zero on the surface S_3 and the shear force $\boldsymbol{\tau}$ is also zero on the surfaces S_1 and S_2, the right-hand side of eq.(2) becomes as follows:

$$-\int_S p\mathbf{n}dS - \int_S \boldsymbol{\tau}dS + \mathbf{g}\int_V \rho dV = -\int_{S_3} p\mathbf{n}_3 dS_3 - \int_{S_3} \boldsymbol{\tau}dS_3 - \int_{S_1} p\mathbf{n}_1 dS_1 \int_{S_2} p\mathbf{n}_2 dS_2 + \mathbf{g}\int_V \rho dV \tag{3}$$

The fluid force acting on the pipe wall $\mathbf{R}$ is represented as follows:

$$\mathbf{R} = \int_{S_3} p\mathbf{n}_3 dS_3 + \int_{S_3} \boldsymbol{\tau}dS_3 \tag{4}$$

Substituting eqs.(2)(3) into eq.(4) and neglecting the term containing $\mathbf{g}$ lead to the following equation.

$$\mathbf{R} = -\frac{\partial}{\partial t}\int_V \rho\mathbf{u}dV - \int_{S_1} p\,\mathbf{n}_1 dS_1 - \int_{S_2} p\,\mathbf{n}_2 dS_2 - \int_{S_1} \rho\,\mathbf{u}_1(\mathbf{u}_1\cdot\mathbf{n}_1)dS_1 - \int_{S_2} \rho\,\mathbf{u}_2(\mathbf{u}_2\cdot\mathbf{n}_2)dS_2 \tag{5}$$

Now, let us apply eq.(5) to a straight pipe volume, a bend pipe volume

and a open end volume shown in Fig.2.

(i) Straight pipe volume

Figure 2(a) shows a straight pipe volume, whose length and flow area are ℓ and A, respectively. Let us assume that ρ is constant in the volume and that $\mathbf{u}$ and p are constant in a cross section and vary linearly along the flow direction. Then, each term of eq.(5) is given as follows:

$$-\frac{\partial}{\partial t}\int_V \rho\mathbf{u}dV = -\frac{\partial}{\partial t}\{A\rho\int_o^\ell |\mathbf{u}|d\ell\} = -A\ell\frac{\partial}{\partial t}\{\rho\frac{u_1+u_2}{2}\}$$

$$= -\frac{A\ell}{2}\{\dot{\rho}(u_1+u_2) + \rho(\dot{u}_1+\dot{u}_2)\} \tag{6}$$

$$-\int_{S_1} p\mathbf{n}_1 dS_1 - \int_{S_2} p\mathbf{n}_2 dS_2 = A(p_1-p_2) \tag{7}$$

$$-\int_{S_1} \rho\mathbf{u}_1(\mathbf{u}_1\cdot\mathbf{n}_1)dS_1 - \int_{S_2} \rho\mathbf{u}_2(\mathbf{u}_2\cdot\mathbf{n}_2)dS_2 = A\rho(u_1^2-u_2^2) \tag{8}$$

Substituting eqs.(6), (7) and (8) into eq.(5) leads to the following equation.

$$R_x = -\frac{A\ell}{2}\{\dot{\rho}(u_1+u_2) + \rho(\dot{u}_1+\dot{u}_2)\} + A(p_1-p_2) + A\rho(u_1^2-u_2^2) \tag{9}$$

(ii) Bend pipe volume

A bend pipe volume is shown in Fig.2(b), in which A, r and ψ denote the flow area, the radius and angle of the bend pipe, respectively. The local xy coordinate system is taken as shown in the figure. Considering that ρ is constant in the volume, the first term of the right-hand side of eq.(5) can be written as follows:

$$\mathbf{R}_1 = -\frac{\partial}{\partial t}\int_V \rho\mathbf{u}dV = -\int_V (\dot{\rho}\mathbf{u}+\rho\dot{\mathbf{u}})dV$$

$$= -Ar\int_{-\psi}^{\psi} (\dot{\rho}\mathbf{u}+\rho\mathbf{a})d\theta \tag{10}$$

in which $\mathbf{a}$ denotes the acceleration vector. The velocity $\mathbf{u}$ and

acceleration $\mathbf{a}$ at the bend pipe can be expressed in terms of the polar coordinate and the orthogonal Cartesian coordinate as follows:

Polar coordinate

$$\mathbf{u} = \begin{Bmatrix} u_r \\ u_\theta \end{Bmatrix} = \begin{Bmatrix} 0 \\ r\dot{\theta} \end{Bmatrix} \tag{11}$$

$$\mathbf{a} = \begin{Bmatrix} a_r \\ a_\theta \end{Bmatrix} = \begin{Bmatrix} -r\dot{\theta}^2 \\ r\ddot{\theta} \end{Bmatrix} \tag{12}$$

Orthogonal Cartesian coordinate

$$\mathbf{u} = \begin{Bmatrix} u_x \\ u_y \end{Bmatrix} = \begin{Bmatrix} -r\dot{\theta}\sin\theta \\ r\dot{\theta}\cos\theta \end{Bmatrix} \tag{13}$$

$$\mathbf{a} = \begin{Bmatrix} a_x \\ a_y \end{Bmatrix} = \begin{Bmatrix} -r\dot{\theta}^2\cos\theta - r\ddot{\theta}\sin\theta \\ -r\dot{\theta}^2\sin\theta + r\ddot{\theta}\cos\theta \end{Bmatrix} \tag{14}$$

$\dot{\theta}$ and $\ddot{\theta}$ can be written in terms of the velocities and accelerations at the inlet and outlet of the bend pipe, assuming that they vary linearly along the flow direction, as follows:

$$\dot{\theta} = \frac{1}{r}\left\{\frac{u_1 + u_2}{2} - \frac{(u_1 - u_2)}{2\psi}\theta\right\} \tag{15}$$

$$\ddot{\theta} = \frac{1}{r}\left\{\frac{\dot{u}_1 + \dot{u}_2}{2} - \frac{(\dot{u}_1 - \dot{u}_2)}{2\psi}\theta\right\} \tag{16}$$

The following relations given in eqs.(11) and (12) are also used to derive the above equations.

$$\dot{\theta} = \frac{u_\theta}{r} \quad , \qquad \ddot{\theta} = \frac{a_\theta}{r}$$

By substituting eqs.(13) and (14) into eq.(10) and using eqs.(15) and

(16), each component of $\mathbf{R}_1$ is calculated as

$$\mathbf{R}_1 = \begin{Bmatrix} (R_1)_x \\ (R_1)_y \end{Bmatrix}$$

$$= \begin{Bmatrix} -\frac{Ar}{\psi}\dot{\rho}(u_1-u_2)(\sin\psi-\psi\cos\psi) \\ +\frac{A\rho}{2}\left[(u_1+u_2)^2\sin\psi+\frac{1}{\psi^2}(u_1-u_2)^2(2\psi\cos\psi+(\psi^2-2)\sin\psi\right] \\ -\frac{Ar\rho}{\psi}(\dot{u}_1-\dot{u}_2)(\sin\psi-\psi\cos\psi) \\ \hline -Ar\dot{\rho}(u_1+u_2)\sin\psi+\frac{A\rho}{\psi}(u_1^2-u_2^2)(\sin\psi-\psi\cos\psi) \\ -Ar\rho(\dot{u}_1+\dot{u}_2)\sin\psi \end{Bmatrix} \tag{17}$$

The second term of the right-hand side of eq.(5) is given by

$$\mathbf{R}_2 = -\int_{S_1} p\,\mathbf{n}_1 dS_1 = -Ap_1\mathbf{n}_1 \tag{18}$$

Thus, the each component of $\mathbf{R}_2$ can be expressed by

$$\mathbf{R}_2 = \begin{Bmatrix} (R_2)_x \\ (R_2)_y \end{Bmatrix} = \begin{Bmatrix} Ap_1\sin\psi \\ Ap_1\cos\psi \end{Bmatrix} \tag{19}$$

Similarly, the components of other terms of eq.(5) can be given as follows:

$$\mathbf{R}_3 = \begin{Bmatrix} (R_3)_x \\ (R_3)_y \end{Bmatrix} = \begin{Bmatrix} Ap_2\sin\psi \\ -Ap_2\cos\psi \end{Bmatrix} \tag{20}$$

$$\mathbf{R}_4 = \begin{Bmatrix} (R_4)_x \\ (R_4)_y \end{Bmatrix} = \begin{Bmatrix} A\rho u_1^2\sin\psi \\ A\rho u_1^2\cos\psi \end{Bmatrix} \tag{21}$$

$$\mathbf{R}_5 = \begin{Bmatrix} (R_5)_x \\ (R_5)_y \end{Bmatrix} = \begin{Bmatrix} A\rho u_2^2\sin\psi \\ -A\rho u_2^2\cos\psi \end{Bmatrix} \tag{22}$$

Finally, each component of the fluid force acting on the bend pipe is expressed as follows:

$$\mathbf{R} = \begin{Bmatrix} R_x \\ R_y \end{Bmatrix}$$

$$= \begin{Bmatrix} -\frac{Ar}{\psi}\dot{\rho}(u_1 - u_2)(\sin\psi - \psi\cos\psi) \\ +\frac{A\rho}{2}\left[(u_1+u_2)^2\sin\psi + \frac{1}{\psi^2}(u_1-u_2)^2(2\psi\cos\psi + (\psi^2-2)\sin\psi)\right] \\ -\frac{Ar\rho}{\psi}(\dot{u}_1 - \dot{u}_2)(\sin\psi - \psi\cos\psi) \\ +A(p_1+p_2)\sin\psi + A\rho(u_1^2+u_2^2)\sin\psi \\ \hline -Ar\dot{\rho}(u_1+u_2)\sin\psi + \frac{A\rho}{\psi}(u_1^2-u_2^2)(\sin\psi - \psi\cos\psi) \\ -Ar\rho(\dot{u}_1+\dot{u}_2)\sin\psi + A(p_1-p_2)\cos\psi \\ +A\rho(u_1^2-u_2^2)\cos\psi \end{Bmatrix} \tag{23}$$

(iii) Open end volume

Figure 2(c) shows a open end volume. Considering that V is equal to zero for a open end volume, eq.(5) is simplified as

$$R_x = -A\{(\rho_e - \rho_o) + u_e^2(\rho_e - \rho_o)\} \tag{24}$$

The blowdown force at an arbitrary location can be obtained from eqs.(9), (23) and (24) by summing up the values pertinent to the volumes concerned. Equations (9), (23) and (24) are given in terms of the local coordinate system denoted by xyz. Therefore, the coordinate transformation to a common global one denoted by XYZ is required to sum up the blowdown forces. The global coordinate fluid force $\mathbf{R}_G$ is related with the local coordinate one $\mathbf{R}_L$ as follows:

$$\mathbf{R}_G = T\,\mathbf{R}_L \tag{25}$$

in which T denotes the matrix for transformation from xyz to XYZ and is given by

$$T = T_\alpha T_\beta T_\gamma \tag{26}$$

T_α, T_β and T_γ in eq.(26) are written as follows:

$$T_\alpha = \begin{pmatrix} \cos\alpha & -\sin\alpha & 0 \\ \sin\alpha & \cos\alpha & 0 \\ 0 & 0 & 1 \end{pmatrix}, \quad T_\beta = \begin{pmatrix} \cos\beta & 0 & -\sin\beta \\ 0 & 1 & 0 \\ \sin\beta & 0 & \cos\beta \end{pmatrix},$$

$$T_\gamma = \begin{pmatrix} 1 & 0 & 0 \\ 0 & \cos\gamma & -\sin\gamma \\ 0 & \sin\gamma & \cos\gamma \end{pmatrix} \tag{27}$$

where α, β and γ denote the angle between x and X axes, etc.

3. Structure of the BLOWDOWN Code

Figure 3 shows the flow chart for the BLOWDOWN code. In the first place, the thermal-hydraulic analysis is carried out by the RELAP4/MOD6 code to obtain the quantities required for calculating the blowdown forces, which are written down in the tape(*), Unit FT11, and are preserved for the calculation of the blowdown forces. In the BLOWDOWN code, the preceding results are read from the tape, Unit FT11, and these are converted into the blowdown forces. The BLOWDOWN code consists of two parts. One is for calculating and editing the blowdown forces and another is for plotting the results. The results are transferred from the former part to the latter one by means of the tape, Unit FT12. This tape is also used as an output tape. In the following are shown the formats of the input and output tapes of the BLOWDOWN codes.

(i) Input tape —— Unit: FT11

Record	Description	Number of words
1	NVOL, NJUN	2
2	TIME, PCR (P(I), I=1, NVOL) (RHO(I), I=1, NVOL),	NVOL × 2 + NJUNC + 3
3 ⋮	Repeat for each time step	

NVOL = number of volumes

NJUN = number of junctions

TIME = time

PCR = pressure at the break end

P(I) = pressure

RHO(I) = density

V(I) = velocity

(ii) Output tape —— Unit: FT12

Record	Description	Number of words
1	Time, NPOIN ((F(I,J), I=1,3), J=1, NPOINT)	NPOINT × 3 + 2
2 ⋮	Repeat for each time step	

NPOINT = number of output points

(*) Tape means magnetic tape, disk and MSS

F(i,J) = blowdown force

i=1 : x-component

i=2 : y-component

i=3 : z-component

4. Input Cards

4.1 Outline of input cards

The following six types of the input cards are required for the BLOWDOWN code.

(1) TITLE cards

These cards give the title for printing and plotting the results.

(2) CONTROL cards

These cards define the basic data for running the program.

(3) VOLUME cards

These cards define the geometries of the volumes.

(4) EDIT cards

These cards define the data for editting the blowdown forces.

(5) PLOT cards

These cards define the data for plotting the blowdown forces.

(6) END card

This card indicates the end of the data.

Each card described above is recognized by the Heading card, which is followed by the data. The characters which describe the type of the card, TITLE, CONTROL, etc., must be written from the first colume in the Heading card. The sequence of the TITLE card through the EDIT cards is arbitrary, but the PLOT cards must be placed after the EDIT cards. Figure 4 shows the input data of the BLOWDOWN code.

4.2 Formats of input cards

The format of each input card is shown in this section.
The signs I, F and A in parentheses indicate the integer variable, real variable and character variable, respectively.

(1) TITLE cards

card no.	columes	variable	entry
1	1 - 5	IHED (A)	Enter the five characters "TITLE"
2	1 - 80	TITLE (A)	Enter the title(*1)

(*1) This title is also used as the titles for printing and plotting the results.

(2) CONTROL cards

card no.	columes	variable	entry
1	1 - 7	IHED (A)	Enter the seven characters "CONTROL"
2	1 - 10	TSTART (F)	Time at the start of the blowdown force calculation (sec)
	11 - 20	TEND (F)	Time at the end of the blowdown force calculation (sec)
	21 - 30	DT (F)	Time step increment (sec)
	31 - 35	KPR(1) (I)	Interval for printing the blowdown force for volume EQ.0: no printing
	36 - 40	KPR(2) (I)	Interval for printing the blowdown force for edit point EQ.0: no printing

(3) VOLUME cards

card no.	columes	variable	entry
1	1 - 6	IHED (A)	Enter the six characters "VOLUME"
2	1 - 5	IVOL (I)	Volume number(*1)
	7	ITYPE (A)	Type of volume EQ.S: straight pipe volume EQ.R: bend pipe volume EQ.*: open end volume
	11 - 15	J1 (I)	Junction number at one end of the volume(*2)
	16 - 20	J2 (I)	Junction number at other end of the volume
	21 - 30	A (F)	Flow area (m^2)
	31 - 40	ELR (F)	Pipe length for the straight pipe volume and bend radius for the bend pipe volume
	41 - 50	PHI (F)	One-half of the angle for the bend pipe volume (degree)
	51 - 60	ALPHA (F)	α } Angles between the local coordinate system and the global global coordinate system (degree)
	61 - 70	BETA (F)	β }
	71 - 80	GAMMA (F)	γ }

The VOLUME data are terminated when IVOL is equal to -1.

Figures 5(a) through 5(c) show the definitions of the notations used in the straight pipe volume, bend pipe volume and open end volume, respectively.

(*1) The volume number of a containment volume must be given for an open end volume.

(*2) The junction number of an open end must be given for an open end volume.

(4) EDIT cards

card no.	colums	variable	entry
1	1 - 4	IHED (A)	Enter the four characters "EDIT"
2	1 - 5	IPOINT (I)	Edit number
	6 - 10	NVOLS (I)	Number of volumes to be added (≦ 50)
	11 - 15	KVOL(1) (I)	Volume number to be added
	16 - 20	KVOL(2) (I)	
	⋮	⋮	
	70 - 80	KVOL(14) (I)	
	(Next card)		
	11 - 15	KVOL(15) (I)	
	16 - 20	KVOL(16) (I)	
	⋮	⋮	

The EDIT data are terminated when IPOINT is equal to -1.

(5) PLOT cards

card no.	colums	variable	entry
1	1 - 4	IHED (A)	Enter the four characters "PLOT"
	6 - 10	KPRINT (I)	Interval for printing the results EQ.0: no printing
	11 - 30	STITLE (A)	Subtitle
	31 - 40	TMIN (F)	Minimum value of abscissa (sec) (*1)
	41 - 50	TMAX (F)	Maximum value of abscissa (sec) (*1)
	51 - 60	VMIN (F)	Minimum value of ordinate (KN) (*1)
	61 - 70	VMAX (F)	Maximum value of ordinate (KN) (*1)
2	1 - 5	IPOINT (I)	Edit number defined in the EDIT cards
	7 - 10	ICOMP (A)	Component of the blowdown force for plotting EQ.X: x-component of the blowdown force (F_X)

(5) PLOT cards (continued)

card no.	columes	variable	entry
2	7 - 10	ICOMP (A)	EQ.Y: y-component of the blowdown force (F_y) EQ.Z: z-component of the blowdown force (F_z) EQ.D: $\sqrt{F_x^2 + F_y^2 + F_z^2}$

The PLOT data are terminated when IPOINT is equal to -1.

(*1) The ranges of abscissa and ordinate are determined automatically, if these data are omitted.

4.3 Limitations of the BLOWDOWN code

The limitations of the BLOWDOWN code are given in the following.

Number of volumes	≦ 200
Number of junctions	≦ 200
Number of output points	≦ 200
Number of volumes per one output point	≦ 50
Number of output steps	≦ 1000
Number of plot points per one figure	≦ 10
Number of components per one plot point	≦ 4
Number of plot lines per one figure	≦ 20

5. Numerical Examples and Discussion

5.1 Saturated steam blowdown

The first numerical example is the problem of saturated steam blowdown from the piping system shown in Fig.6, the results of which were given by Moody.[6] The flow area and length of the piping are assumed to be 0.06452 m^2(100 in^2) and 48.77 m(160 ft), respectively. The piping is composed of three segments of the straight piping, the lengths of which are 19.51 m(64 ft), 9.75 m(32 ft) and 19.51 m(64 ft), respectively. Compared with that of piping, the volume of a source tank is large enough to keep its pressure constant during the blowdown. The source tank and the piping contain saturated steam at 6.89 MPa (1000 psia). As shown in Fig.6, the system was modeled with 21 junctions and 22 volumes.

Three critical flow models were used in the thermal-hydraulic analysis by the RELAP4/MOD6 code. These were the Moody model, the homogeneous equilibrium model and the sonic model. Figures 7(a) through 7(c) show the blowdown forces obtained from the RELAP4/BLOWDOWN. In these figures, the solid line and the broken like denote the results of the detailed analysis using the method of characteristics and that of the simplified analysis, both of which were obtained by Moody, respectively. The results of the present analysis using the Moody model and the homogeneous equilibrium model indicate relatively good agreement with that of the detailed analysis by Moody. On the other hand, the present analysis using the sonic model gives the lower value of Fl than the detailed analysis by Moody. This may be due to the reason that the exit pressure is lower in the sonic model than in the detailed analysis by Moody.

5.2 Edwards' pipe

Edwards[7] performed a subcooled water blowdown test and measured the pressures, void fraction and blowdown force. Figure 8 shows the analytical model which consists of 17 volumes and 16 junctions. Initial pressure was 6.99 MPa (1000 psig). The uniform distribution of the initial temperature of 241.6°C (467°F) was reported in the Edwards' paper. It was, however, pointed out that there was large difference of the pressure between the test and the analysis using the temperature

distribution reported by Edwards. Therefore, the distribution of the initial temperature shown in Fig.8[8] was used in the present analysis. The break area ratio was 87 percents.

Before calculating the blowdown force, the thermal-hydraulic analysis was carried out using the RELAP4/MOD6 code. Figures 9(a) and 9(b) show the comparison of the pressure between the present analysis and the Edwards' test. In the figures, HF-HEM indicates that the Henry-Fauske model and the homogeneous equilibrium model were used as the critical flow models in the subcooled region and the saturated region, respectively, while HF-M indicates that the Henry-Fauske model and the Moody model were used as the critical flow models in the subcooled region and the saturated region, respectively. In the present analysis, the discharge coefficient C_D was taken as equal to 1.0. The results of the present analysis cannot, however, simulate the rapid decrease of pressure below saturated pressure and the gradual recovery to saturated pressure, as shown in the result of GS7.

Figure 10 shows the comparison of the blowdown force between the present analysis and the Edwards' test. The results obtained from the present analyses using the HF-HEM model and the HF-M model agree quite well with the Edwards' test data.

5.3 Hanson's pipe

Hanson[9] inplemented the subcooled water blowdown tests under the room temperature condition and obtained the blowdown force. He also carried out the analysis using the water hammer code.

Figure 11 shows the analytical model which consists of 17 volumes and 16 junctions. The initial pressure of 15.09 MPa (2189 psia) and the initial temperature of 100°C were used in the present analysis. First of all, it was studied to what extent the RELAP4/MOD6 code can deal with the wave propagation phenomenon. Figure 12 shows the time histories of the pressure at Vol.1, Vol.10 and Vol.13. Three types of the critical flow model were employed in the RELAP4/MOD6 analysis. These were the HF-HEM model, the HF-M model and the inertia model, IN. The results obtained from the DEPCO-MULTI code[10] are depicted in the figure for comparison. The DEPCO-MULTI code is able to deal with the wave propagation phenomenon such as a water hammer exactly since this code employs the method of characteristics. Compared with the

DEPCO-MULTI code, the RELAP4/MOD6 code does not give sharp pressure change.

Figure 13 shows the comparison of the blowdown force between the present analysis and the Hanson's test. Good agreement is not found between the present analysis and the Hanson's test because the RELAP4/MOD6 code cannot represent exactly the pressure change due to a water harmmer.

The contribution of the wave thrust caused by the pressure propagation to the total blowdown force is much larger in the high subcooled water blowdown than in the low subcooled water blowdown.
Therefore, such a thermal-hydraulic analysis code as DEPCO-MULTI should be used in order to obtain the accurate blowdown force of high subcooled water.

5.4 Pipe rupture test performed at the Japan Atomic Energy Research Institute

A pipe rupture test, RUN No.5509, was performed at the Japan Atomic Energy Research Institute (= JAERI) to obtain the blowdown force under the PWR LOCA conditions. Figure 14 shows the schematic figure of the test. The 4-inch pipe was used as a test pipe. An instantaneous pipe rupture was simulated by breaking the rupture disk attached to the end of the test pipe. The blowdown force was measured by the load cell installed at the elbow adjacent to the break end. The locations of the pressure transducers and thermocouples are also shown in the figure. Table 1 shows the initial pressure, the initial temperature and the break area ratio of the rupture disk.

Figure 15 shows the analytical model composed of 15 volumes and 14 junctions. The heating-up line connected to the pressure vessel was not considered in the present model because its volume was too small to have an effect on the short-term blowdown characteristics.

The thermal-hydraulic analysis was performed with the RELAP4/MOD6 code using the HF-HEM model and the HF-M model. Figures 16(a) and 16(b) show the comparison of the pressure between the present analysis and the JAERI's test. The analytical results of both models are in good agreement with those of the JAERI's test. The analysis is also able to simulate the pressure oscillation due to the water hammer which appears at the pressure transducers of PU113 and PU105.

In the calculation of blowdown force, two models were employed to represent the elbow adjacent to the break end. One was Bend Model, in which a bend pipe volume was used to represent the elbow and the blowdown force was calculated from eq.(23). The other was Straight Model, in which a straight pipe volume was used to represent the elbow and the blowdown force was calculated from eq.(9). Namely, the momentum variation at the elbow is not taken into account in Straight Model. The computer codes such as PRTHRUST-J1 and REPIPE uses the latter model, which is less exact than the former one from a theoretical point of view.

Figures 17(a) and 17(b) show the comparison of the blowdown force between the present analysis and the JAERI's test. These figures indicate that the HF-HEM model gives better agreement with the JAERI's test than the HF-M model. Compared the result of Bend Model with that of Straight model, the former is larger than the latter by the amount of the fluid force due to the momentum change at the elbow.
More quantitive discussion is given for the difference between the results of Bend Model and Straight Model. Figure 18 gives the two schematic models, in which Model I and Model II correspond to Straight Model and Bend Model, respectively. In the Model I, the blowdown force is assumed to be measured at the end of a straight pipe. On the other hand, the blowdown force is assumed to be measured at the bend pipe adjacent to the break end in the Model II. The flow rate W_e, specific weight γ_e, pressure p_e and flow area A_e at the exit are assumed to be the same in both models. Let us consider a steady state for simplification. The total blowdown force of the Model I is the sum of the pressure term and the momentum term as follows:

$$F_I = A_e (p_e - p_o) + \frac{W_e^2}{A_e \gamma_e g} \tag{28}$$

In the total blowdown force of the Model II, the fluid force caused by the momentum change at the bend pipe must be added to eq.(28).
Thus, the total blowdown force of the Model II is given by

$$F_{II} = F_I + \frac{W_b^2}{A_b \gamma_b g} \sin\alpha \qquad (0 \leqq \alpha \leqq 180°) \tag{29}$$

in which α is the angle of the bend pipe as shown in the figure. Eqs.(28) and (29) indicate that F_{II} is larger than F_I. Now, let us consider a 90-degree elbow which has the same flow area as the exit and is located nearly at the exit. Then, the following relations are established.

$$A_e = A_b \quad , \quad W_e \doteqdot W_b \quad , \quad \gamma_e \doteqdot \gamma_b \tag{30}$$

Considering eqs.(28), (29) and (30), the momentum term of F_{II} is formally twice as much as that of F_I. The difference between Straight Model and Bend Model shown in Figs.17(a) and 17(b) can be explained by the above discussion.

6. Concluding Remarks

In this paper is described the outline of the BLOWDOWN code for the calculation of the blowdown force, which is a post-processor of the RELAP4/MOD6 code. Some numerical examples are also presented to show the effectiveness and limitation of the BLOWDOWN code. The following conclusions are obtained from the analyses.

(1) The accurate blowdown force can be calculated from the BLOWDOWN code, if the thermal-hydraulic analysis by the RELAP4/MOD6 code gives good agreement with other calculations or experiments as to pressures.

(2) The accurate pressures cannot be obtained from the RELAP4/MOD6 code, if the effect of the pressure wave is primarily important as shown in the results of the Hanson's pipe. In such a case, the blowdown force should be calculated using the results obtained from the thermal-hydraulic code based on the method of characteristics.

(3) The fluid force due to the momentum change at the bend pipe should be taken into account in the blowdown force analysis including the bend pipe.

ACKNOWLEDGEMENT

The authors wish to make their grateful acknowledgement to Dr. S. Miyazono, Chief of the Mechanical Strength and Structure Laboratory at JAERI, and Messers. T. Yano and T. Isozaki, collegues of one of the authors. Acknowledgement is also due to Mr. D. Hiroshe and Miss C. Ino, staffs of Century Research Center Corporation, for their aid in developing the BLOWDOWN code.

6. Concluding Remarks

In this paper is described the outline of the BLOWDOWN code for the calculation of the blowdown force, which is a post-processor of the RELAP4/MOD6 code. Some numerical examples are also presented to show the effectiveness and limitation of the BLOWDOWN code. The following conclusions are obtained from the analyses.

(1) The accurate blowdown force can be calculated from the BLOWDOWN code, if the thermal-hydraulic analysis by the RELAP4/MOD6 code gives good agreement with other calculations or experiments as to pressures.

(2) The accurate pressures cannot be obtained from the RELAP4/MOD6 code, if the effect of the pressure wave is primarily important as shown in the results of the Hanson's pipe. In such a case, the blowdown force should be calculated using the results obtained from the thermal-hydraulic code based on the method of characteristics.

(3) The fluid force due to the momentum change at the bend pipe should be taken into account in the blowdown force analysis including the bend pipe.

ACKNOWLEDGEMENT

The authors wish to make their grateful acknowledgement to Dr. S. Miyazono, Chief of the Mechanical Strength and Structure Laboratory at JAERI, and Messers. T. Yano and T. Isozaki, collegues of one of the authors. Acknowledgement is also due to Mr. D. Hiroshe and Miss C. Ino, staffs of Century Research Center Corporation, for their aid in developing the BLOWDOWN code.

REFERENCES

[1] EG & G IDAHO, INC., "RELAP4/MOD6 —— A Computer Program for Transient Thermal-Hydraulic Analysis of Nuclear Reactors and Related Systems, User's Manual", CDAP TR003, 1978.

[2] Miyazaki, N., Kurihara, R., Kato, R., Isozaki, T. and Ueda, S., "PRTHRUST-J1 code for Calculation of Blowdown Thrust Force and Its Experimental Verification", Nuclear Engineering and Design, Vol.64, 1981, p.389.

[3] Hsu, M., Weisman, J. and Redmond, J.W., "An Evaluation of Time-Dependent Loading Analysis on a Piping Network Using RELAP4/REPIPE", Nuclear Technology, Vol.59, 1981, p.58.

[4] Strong, B.R.Jr. and Bahiere, R.J., "Pipe Rupture and Steam/Water Hammer Design Loads for Dynamic Analysis of Piping Systems", Nuclear Engineering and Design, Vol.45, 1978, p.419.

[5] Moody, F.J., "Time-Dependent Pipe Forces Caused by Blowdown and Flow Stoppage", Journal of Fluid Engineering, Trans. ASME Series I, Vol.95, p.422.

[6] Moody, F.J., "Fluid Reaction and Impingement Loads", Nuclear Power Plant, 1973, p.219.

[7] Edwards, A.R. and O'Brien, T.P., "Studies of Phenomena Connected with Depressurization of Water Reactors", Journal of British Nuclear Engineering Society, Vol.9, 1970, p.58.

[8] Moore, K.V., Slater, C.E., Ybarrondo, L.J. and Gruen, G.E., "Momentum Flux Hydarulic Terms in Decompression Codes", Conf-730304-10, 1973.

[9] Hanson, G.H., "Subcooled-Blowdown Forces on Reactor-System Components: Calculational Method and Experimental Confirmation", IN-1354, 1970.

[10] Namatame, K. and Kobayashi, K., "Subcooled Decompression Analysis in PWR LOCA", Journal of Heat Transfer, Tans. ASME, Series C, Vol.98, 1976, p.12.

Nomenclature

A	= flow area
$\mathbf{a}$	= acceleration vector
$\mathbf{g}$	= unit vector orientation for gravitation
ℓ	= length of control volume
$\mathbf{n}$	= outward unit vector normal to surface S
p	= pressure
$\mathbf{R}$	= blowdown force
S	= boundary of control volume
t	= time
$\mathbf{u}$	= flow velocity vector
V	= control volume
W	= flow rate
ψ	= angle of bend pipe
ρ	= fluid density
$\boldsymbol{\tau}$	= shear force vector at the boundary of fluid
λ	= coefficient of thermal conductivity
μ	= coefficient of viscosity
$\gamma\theta$	= polar coordinate system
XYZ	= global coordinate system
xyz	= local coordinate system

Subscripts and Other Symbols

0	= atomosphere
b	= bend pipe
e	= pipe exit
$\dot{(\ )},\ddot{(\ )}$	= differentiation with respect to time t

Table 1 Test Conditions of Pipe Rupture Test at JAERI

RUN No.		5509
Pressure (MPa)		15.40
Temperature (°C)	TU101	319.4
	TU102	320.2
	TU120	319.4
	TU121	317.6
	TU122	316.7
	TU125	315.8
Break Area Ratio		78.6 %

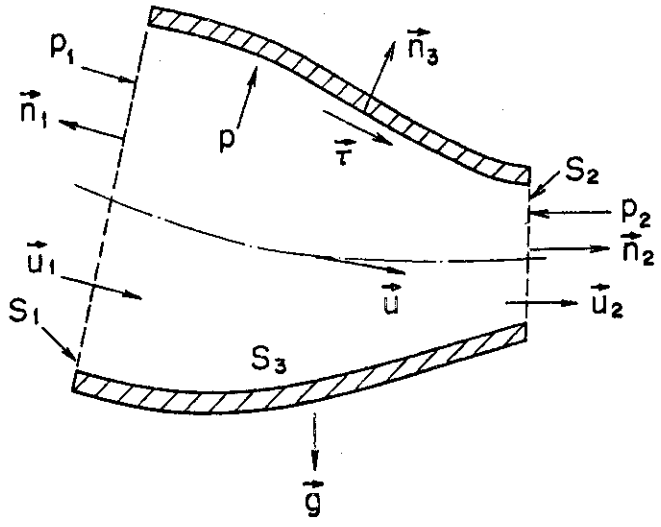

Fig. 1 Flow and Force Elements for a Control Volume

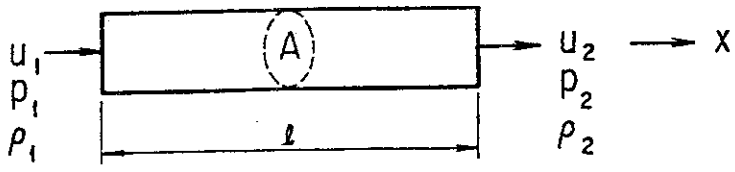

(a)

(a) Straight Pipe Volume

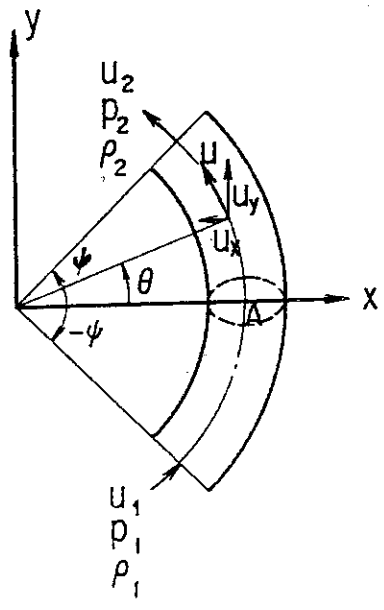

(b)

(b) Bend Pipe Volume

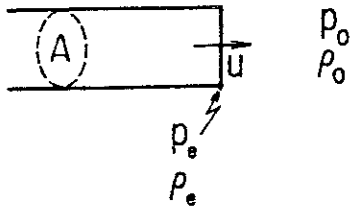

(c)

(c) Open End Volume

Fig. 2 Control Volumes Contained in the BLOWDOWN Code

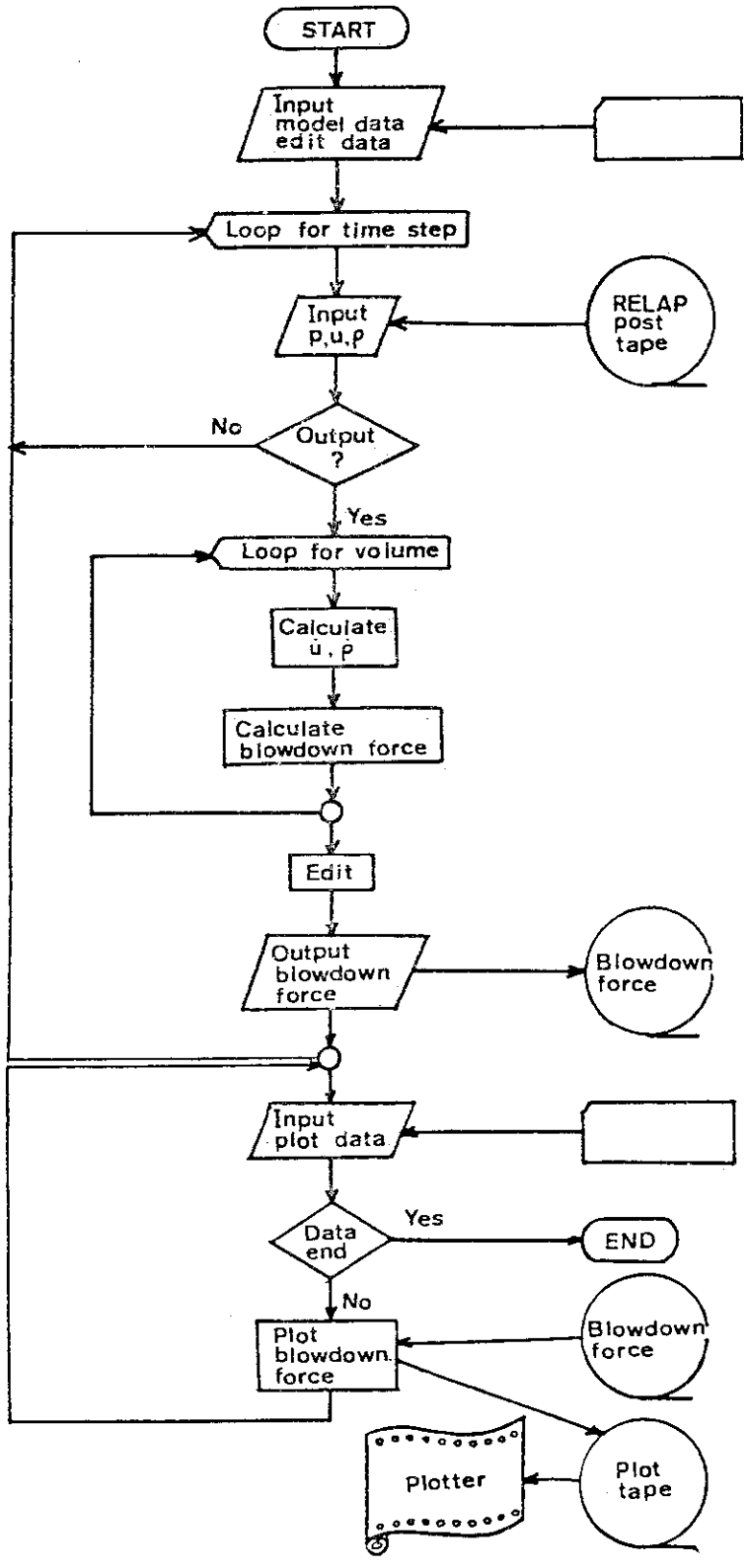

Fig. 3 Flowchart for the BLOWDOWN Code

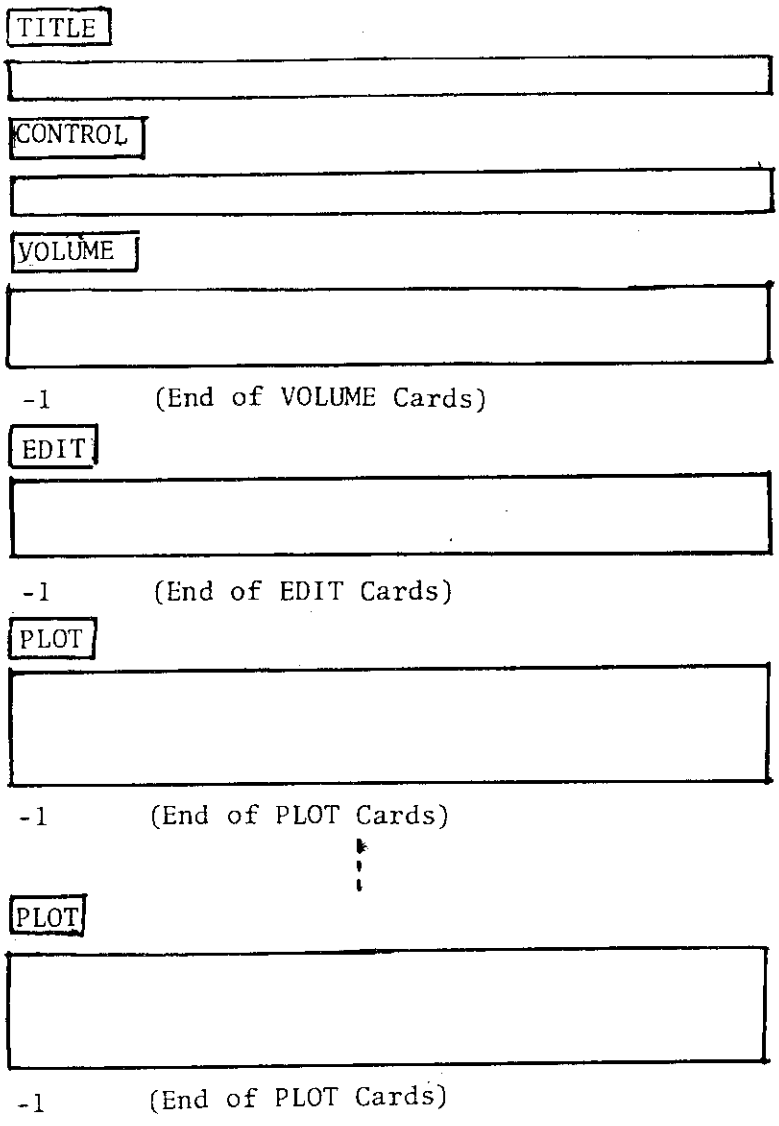

Fig. 4 Sequence of Input Cards

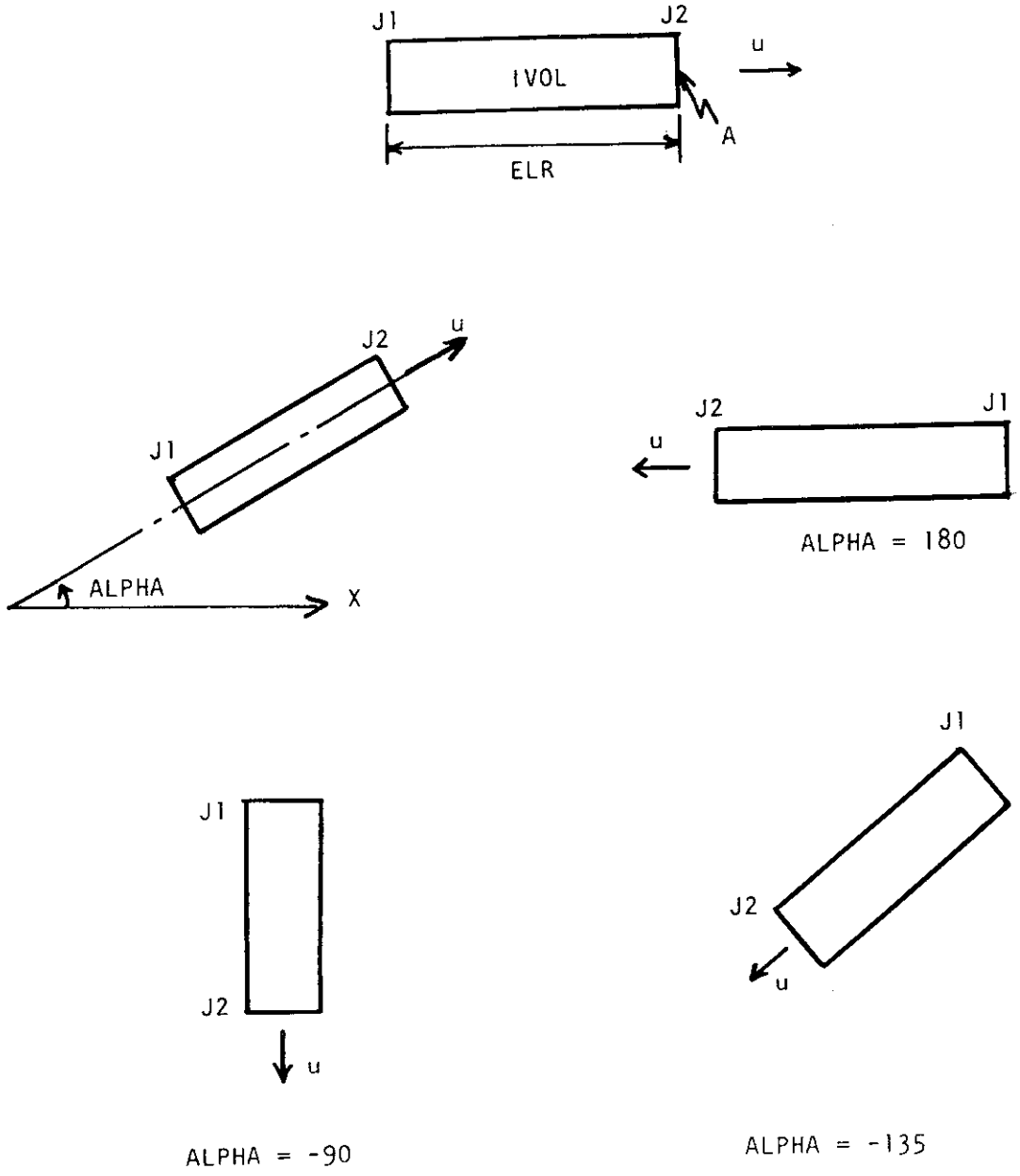

Fig. 5 Definitions of Notations
(a) Straight Pipe Volume

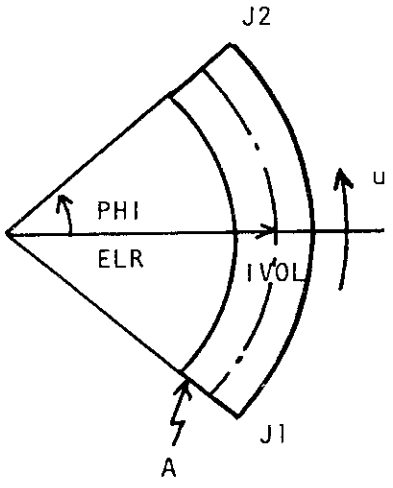

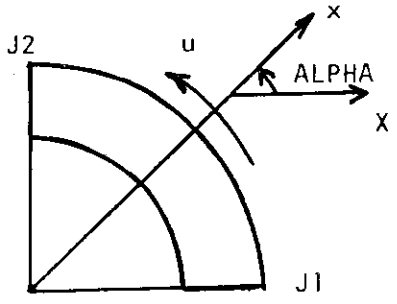

ALPHA = 45 , GAMMA = 0

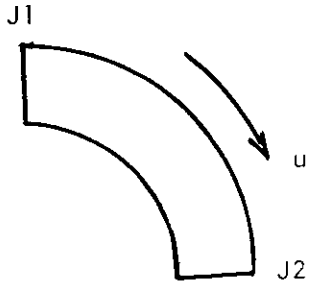

ALPHA = 45 , GAMMA = 180

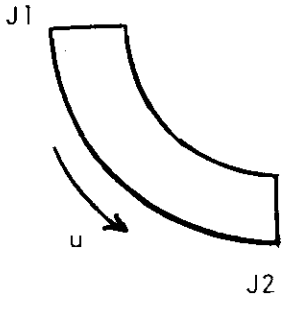

ALPHA = -135 , GAMMA = 0

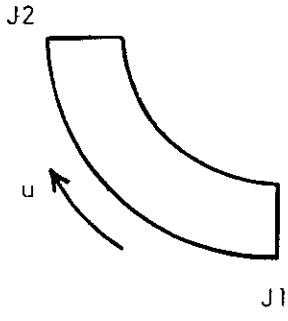

ALPHA = -135 , GAMMA = 180

(b) Bend Pipe Volume

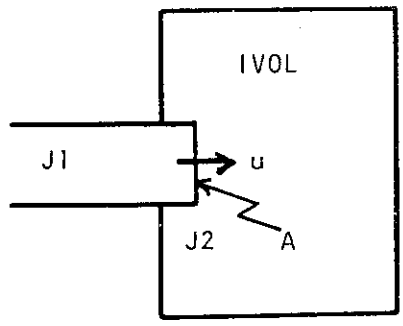

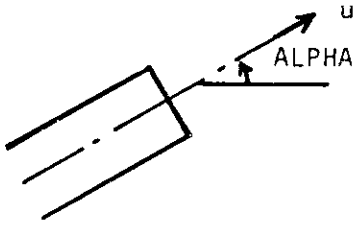

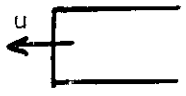

ALPHA = 180

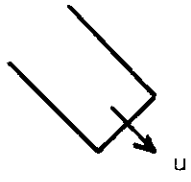

ALPHA = -45

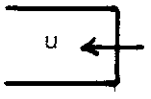

ALPHA = 180

(c) Open End Volume

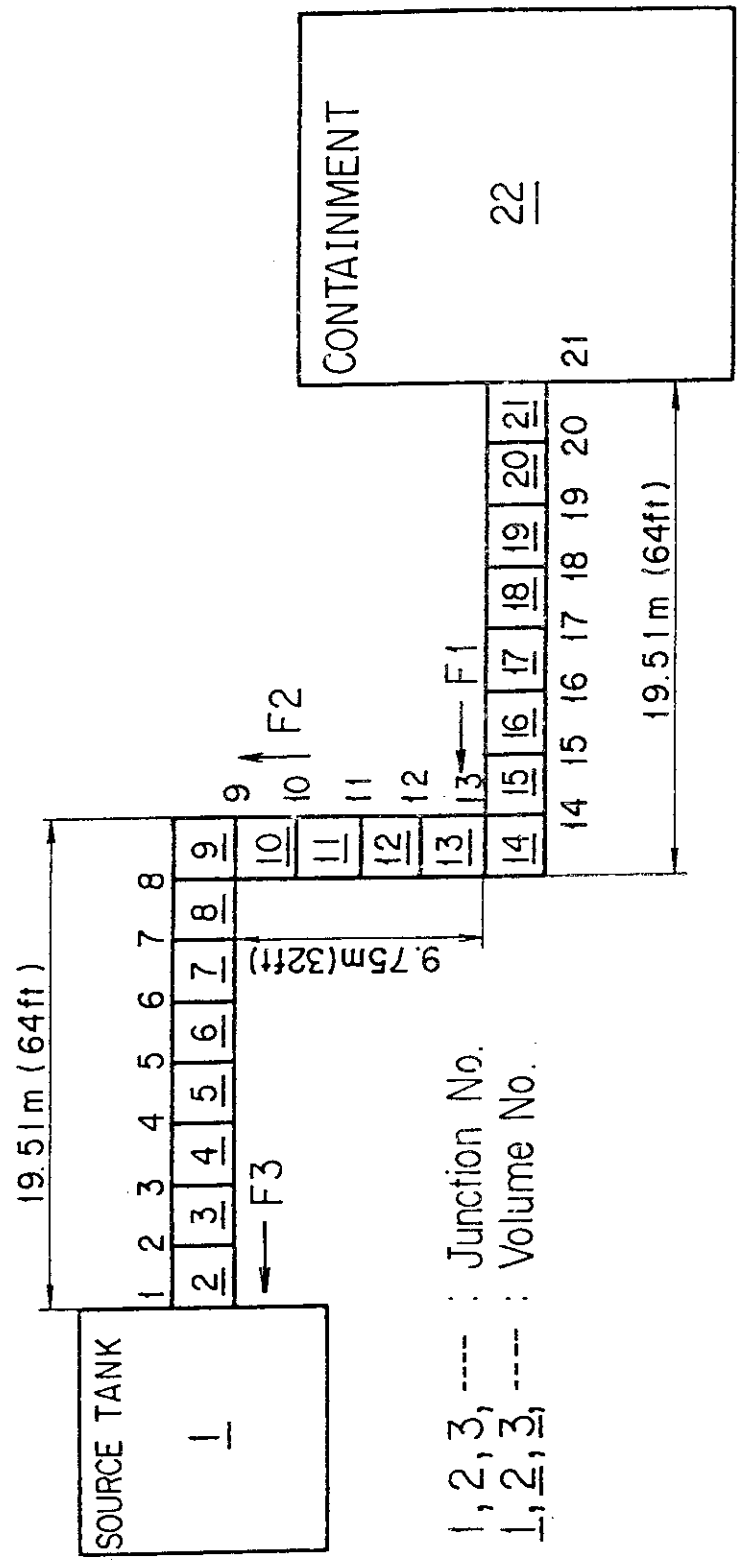

Fig. 6 Volume Division of Saturated Steam Blowdown

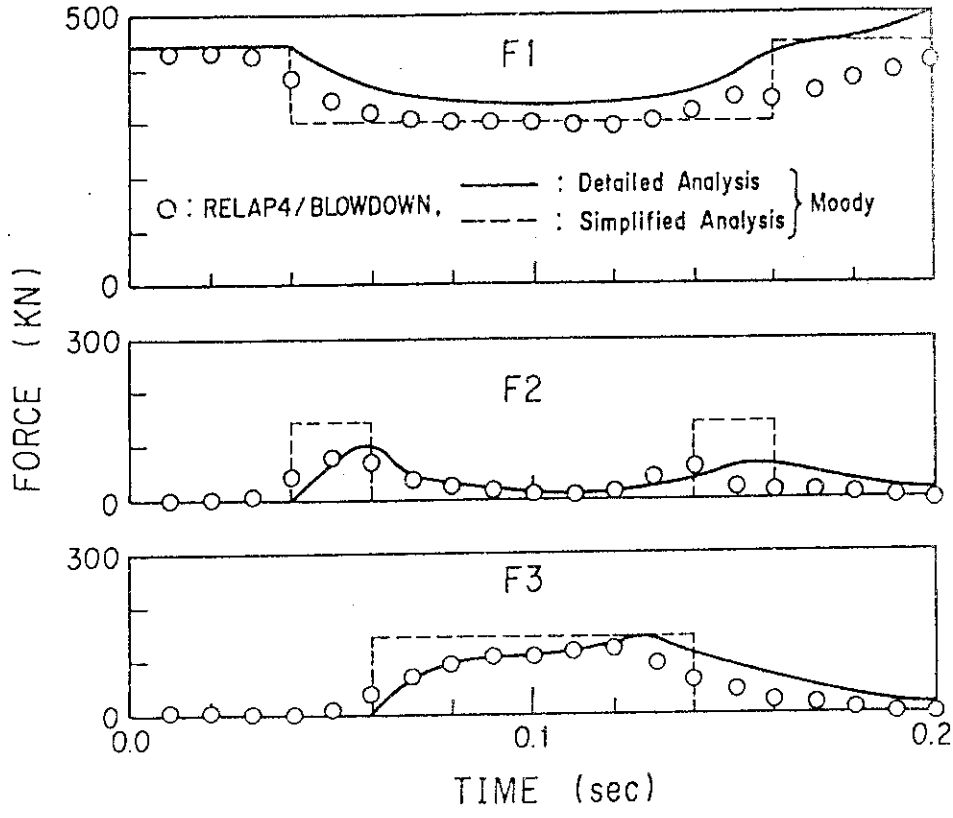

(a) HEM Model

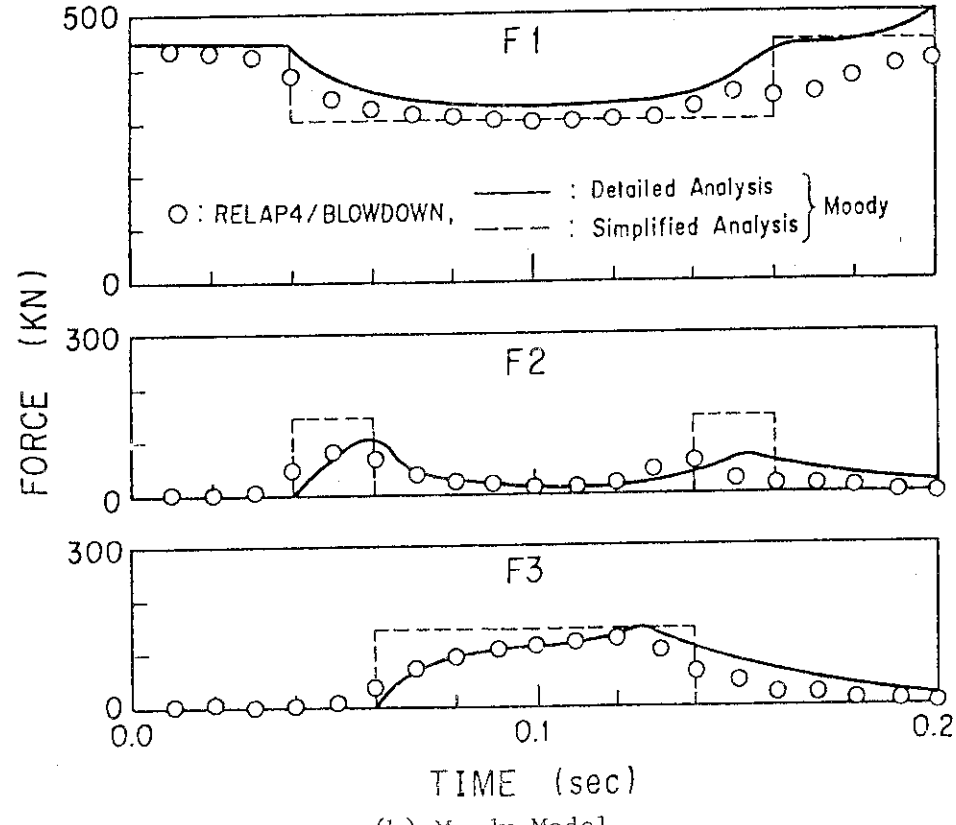

(b) Moody Model

Fig. 7 Comparison of Blowdown Force between RELAP4/BLOWDOWN Analysis and Moody's Analysis

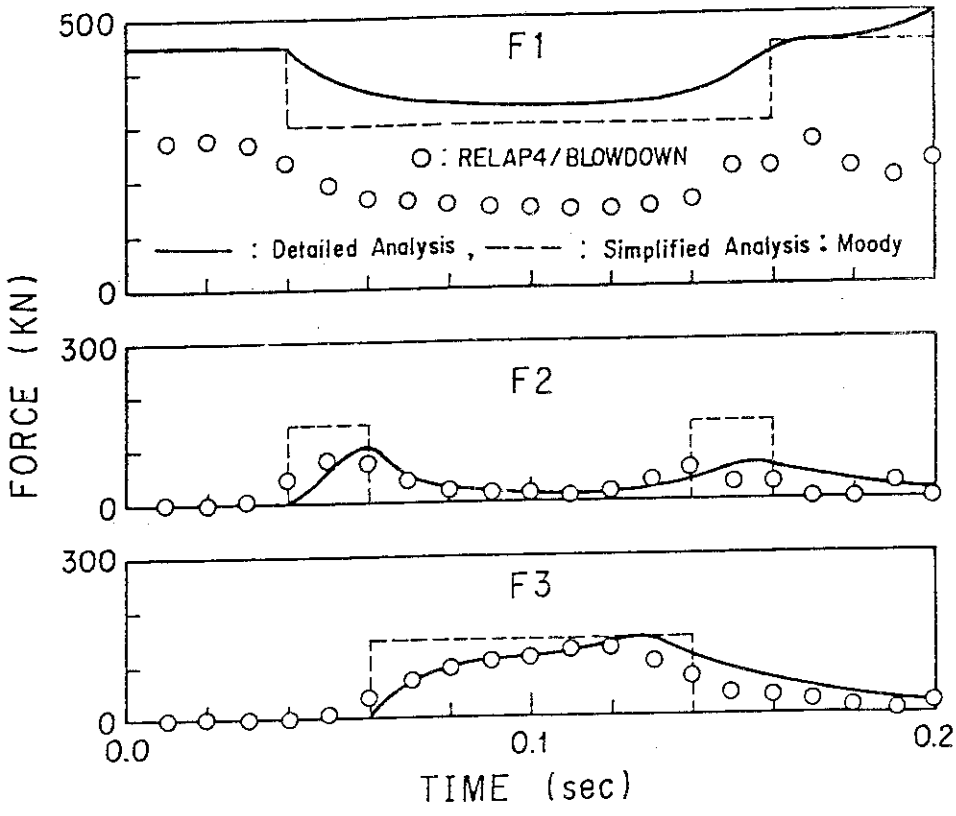

(c) Sonic Model

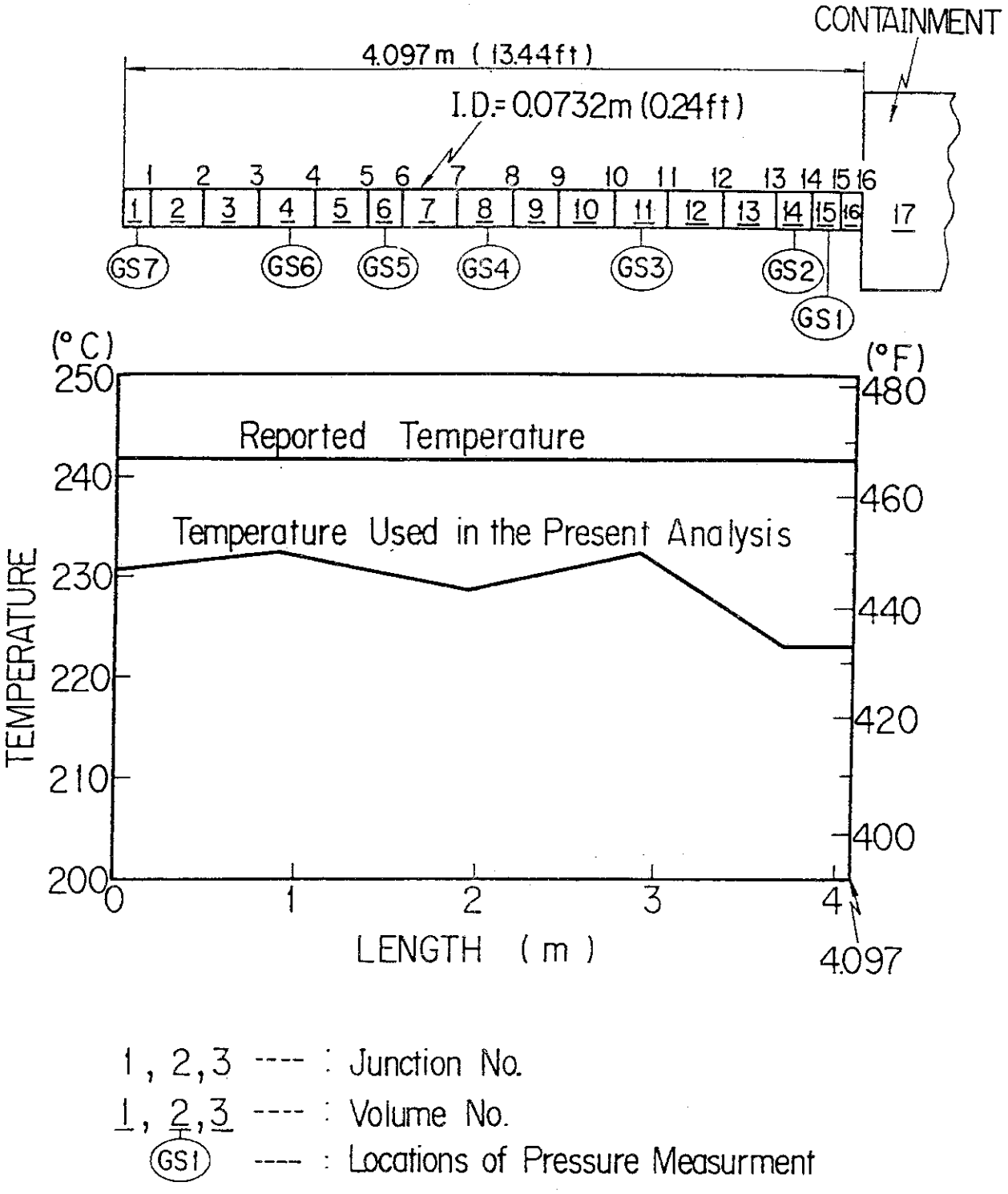

Fig. 8 Volume Division and Initial Temperature Distribution of Edwards' Pipe

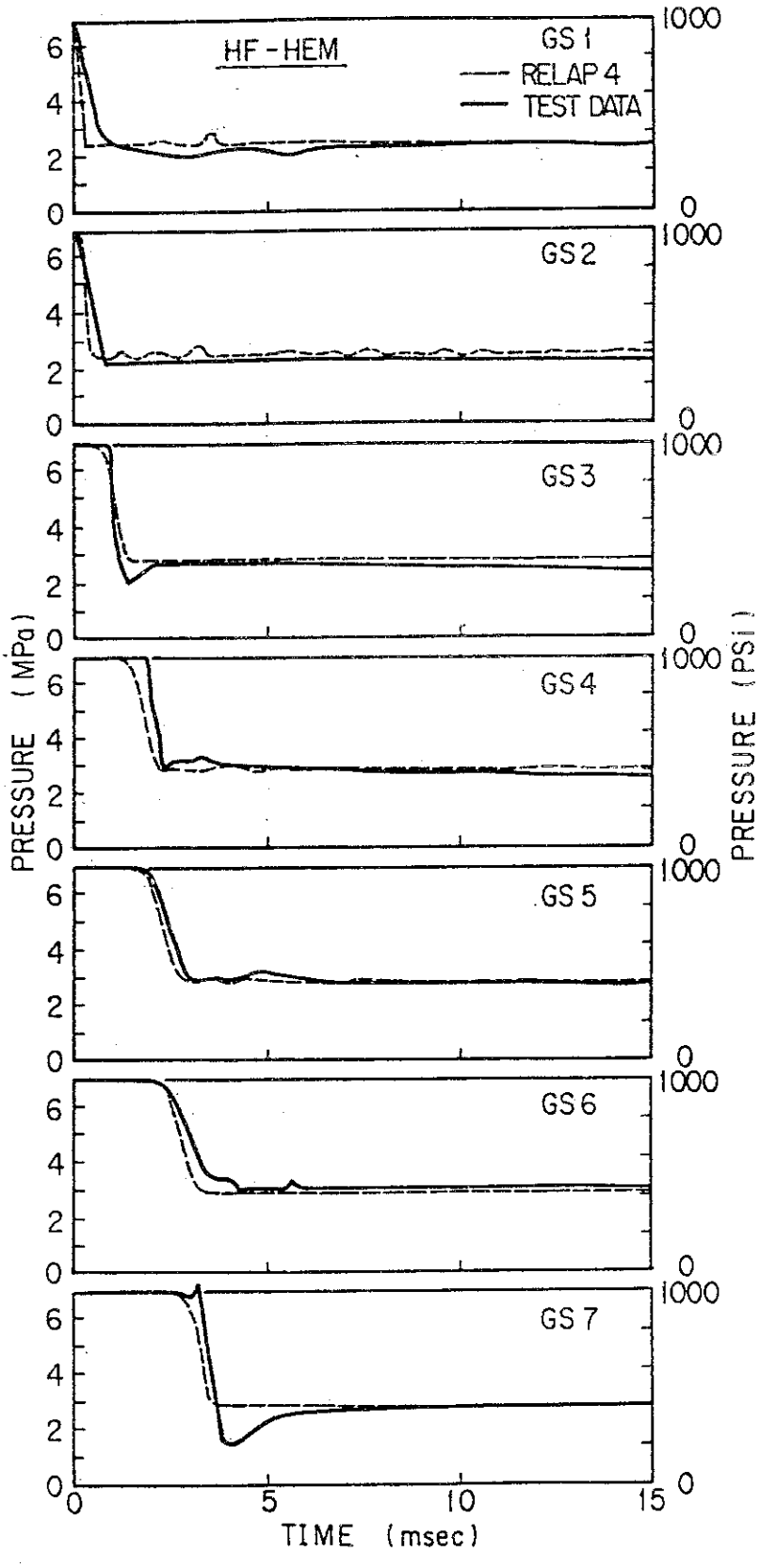

(a) HF-HEM Model

Fig. 9 Comparison of Pressures between RELAP4 Analysis and Edwards' Test

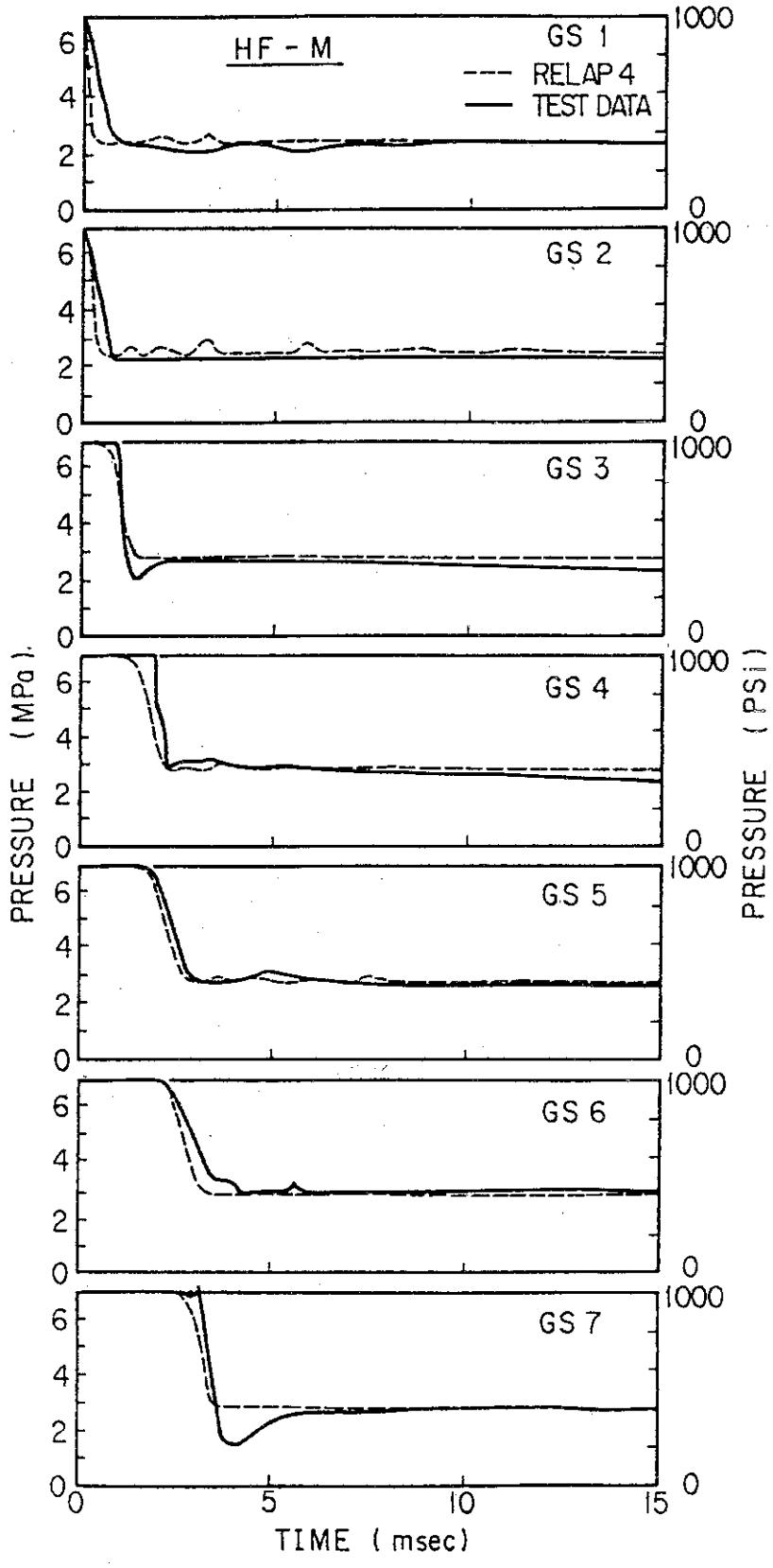
HF - M
GS 1
RELAP 4
TEST DATA
GS 2
GS 3
GS 4
GS 5
GS 6
GS 7
PRESSURE (MPa)
PRESSURE (PSi)
TIME (msec)
0
2
4
6
0
5
10
15
0
1000

(b) HF-M Model

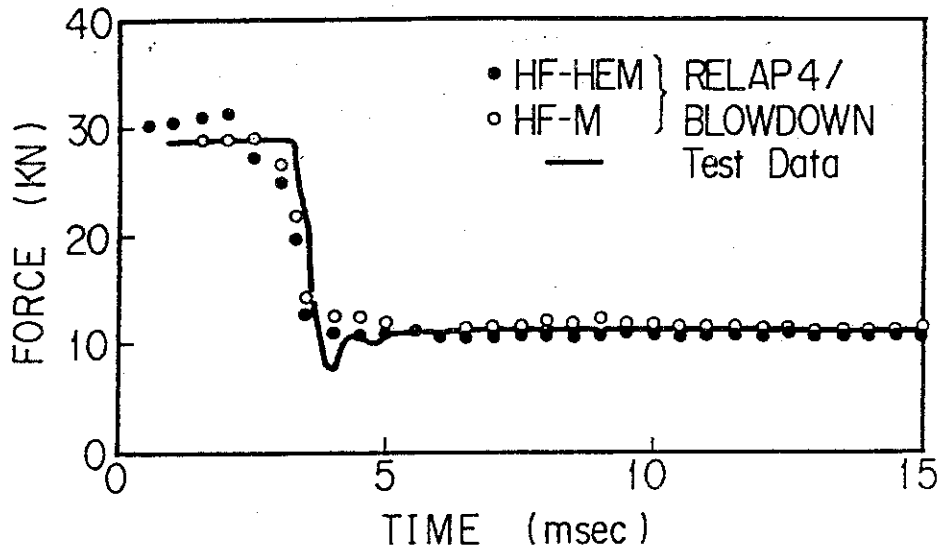

Fig.10 Comparison of Blowdown Force between RELAP4/BLOWDOWN Analysis and Edwards' Test

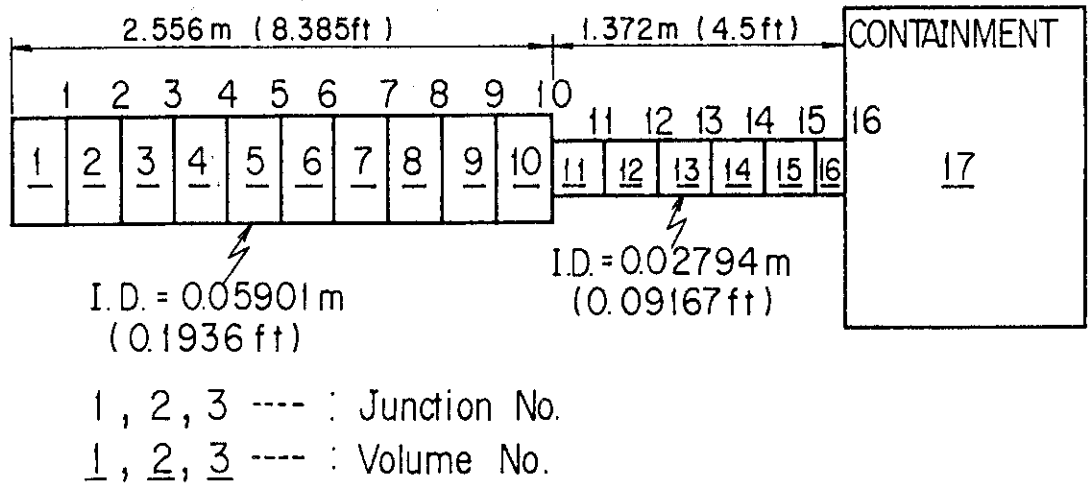

Fig.11 Volume Division of Hanson's Pipe

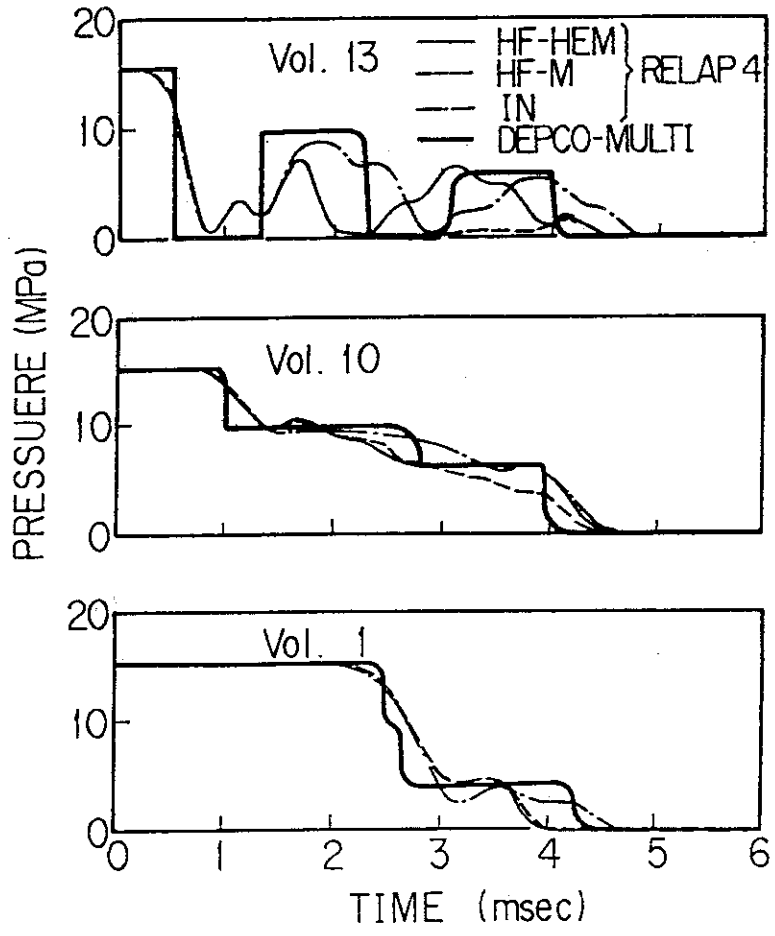

Fig.12 Comparison of Pressures between RELAP4 Analysis and DEPCO-MULTI Analysis

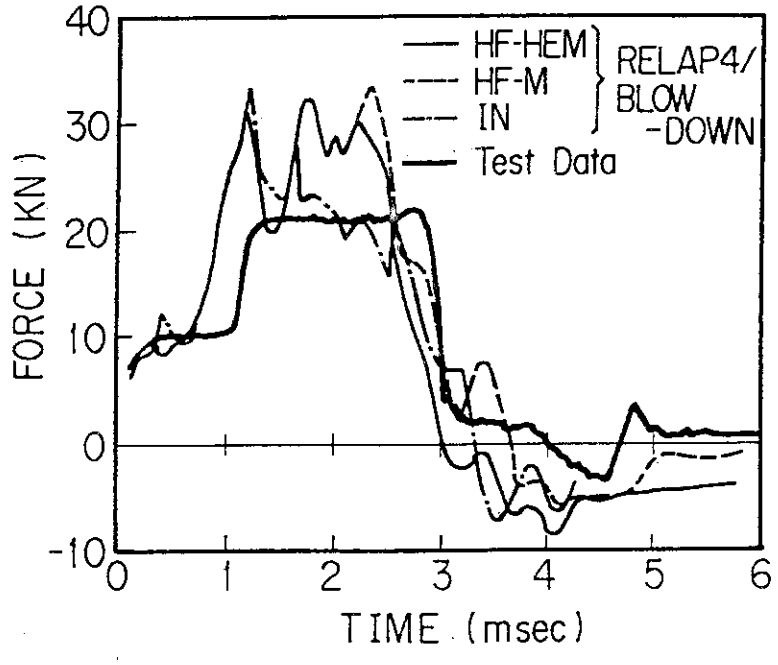

Fig.13 Comparison of Blowdown Force between RELAP4/BLOWDOWN Analysis and Hanson's Test

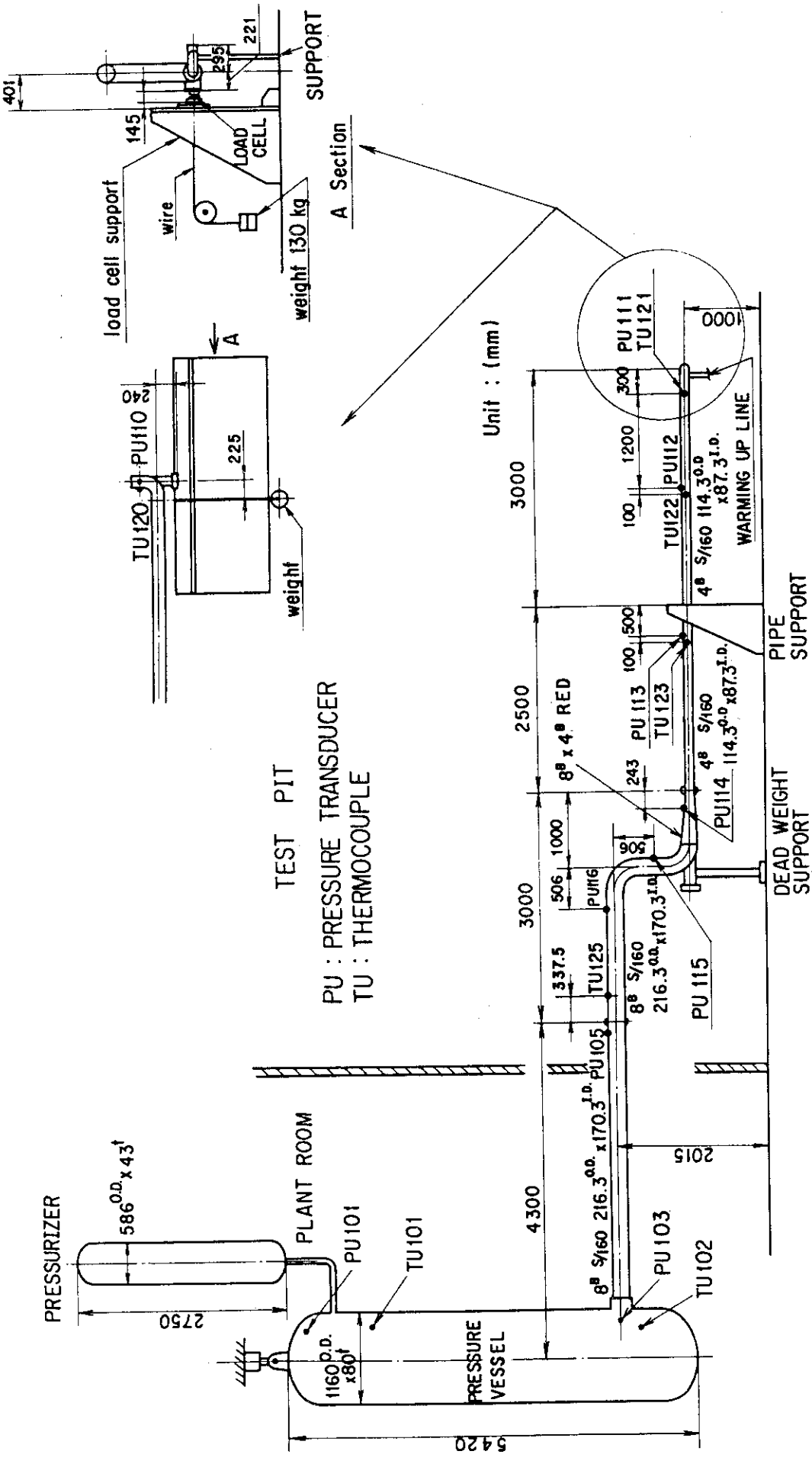

Fig.14 Schematic Figure of Pipe Rupture Test at JAERI

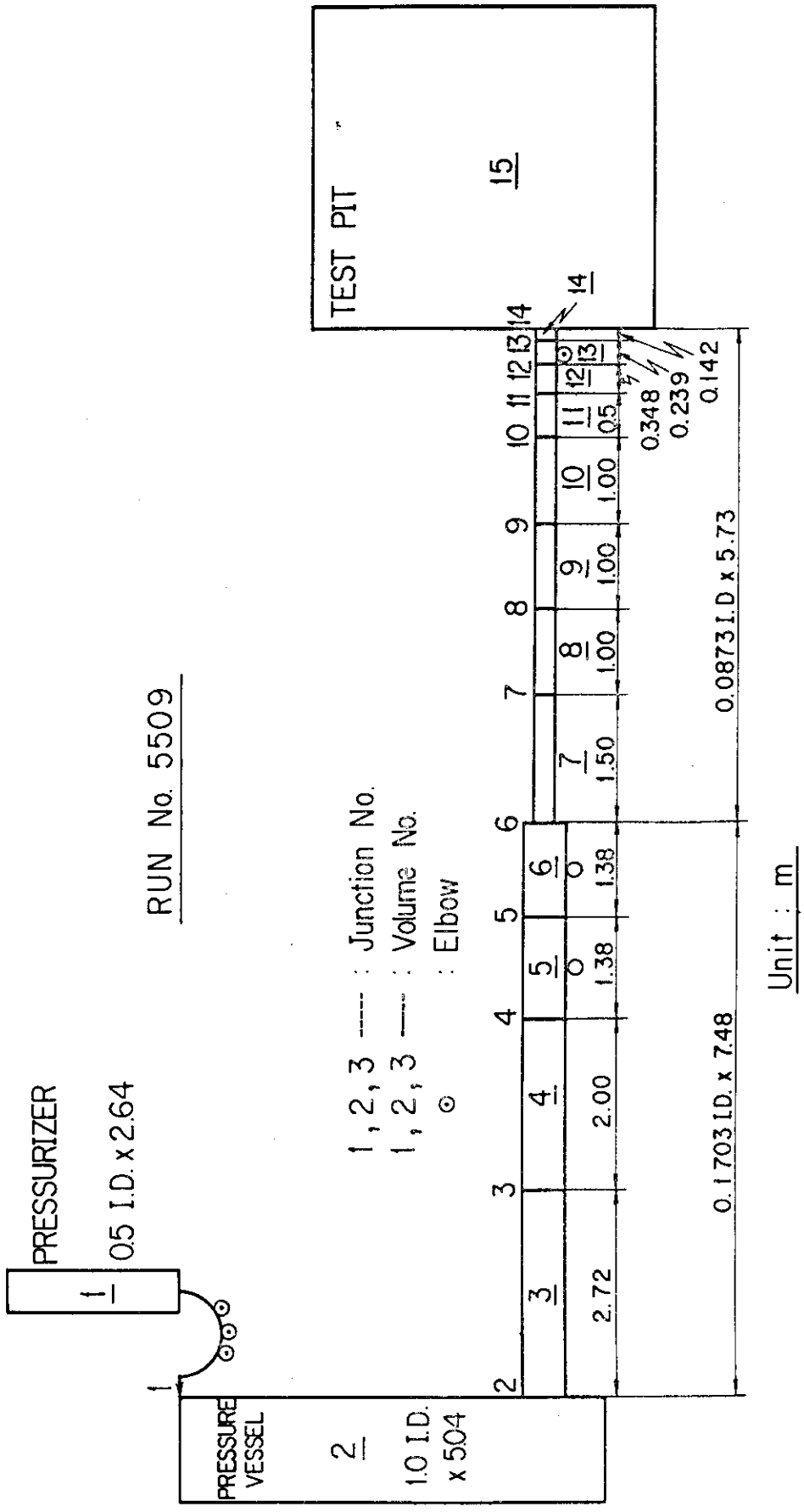

Fig.15 Volume Division of JAERI's Test

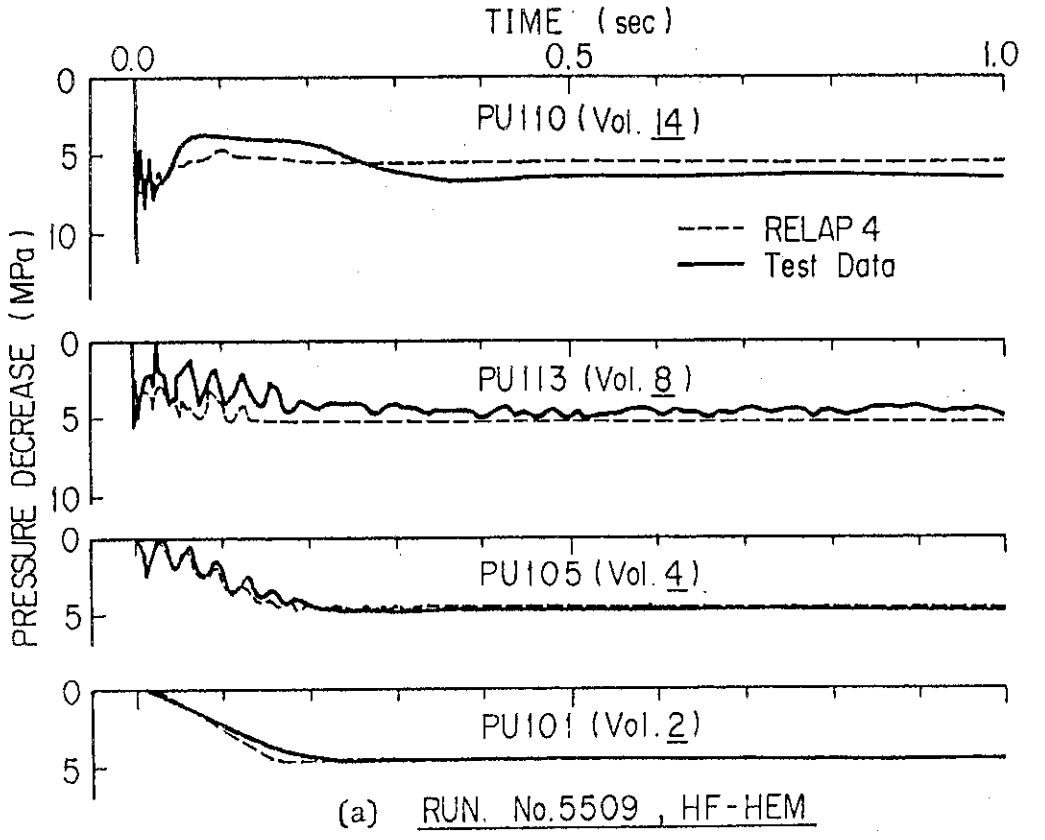

(a) HF-HEM Model

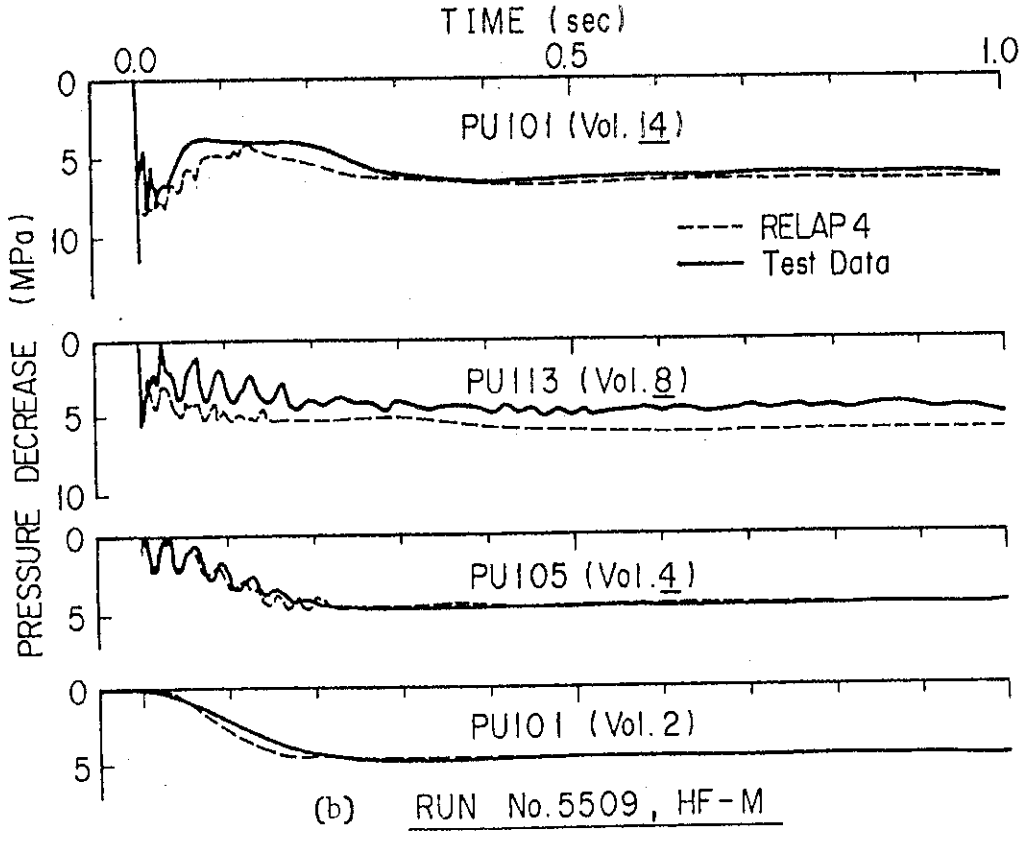

(b) HF-M Model

Fig.16 Comparison of Pressures between RELAP4 Analysis and JAERI's Test

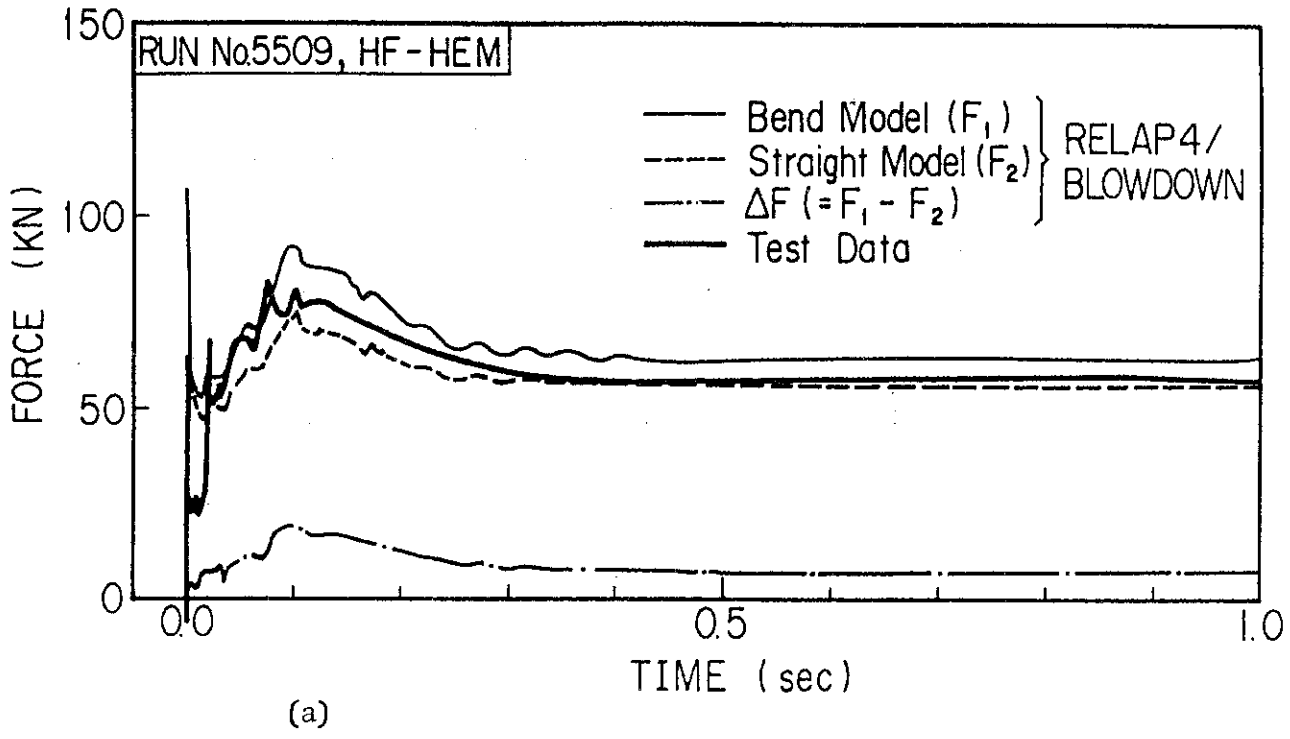

(a) HF-HEM Model

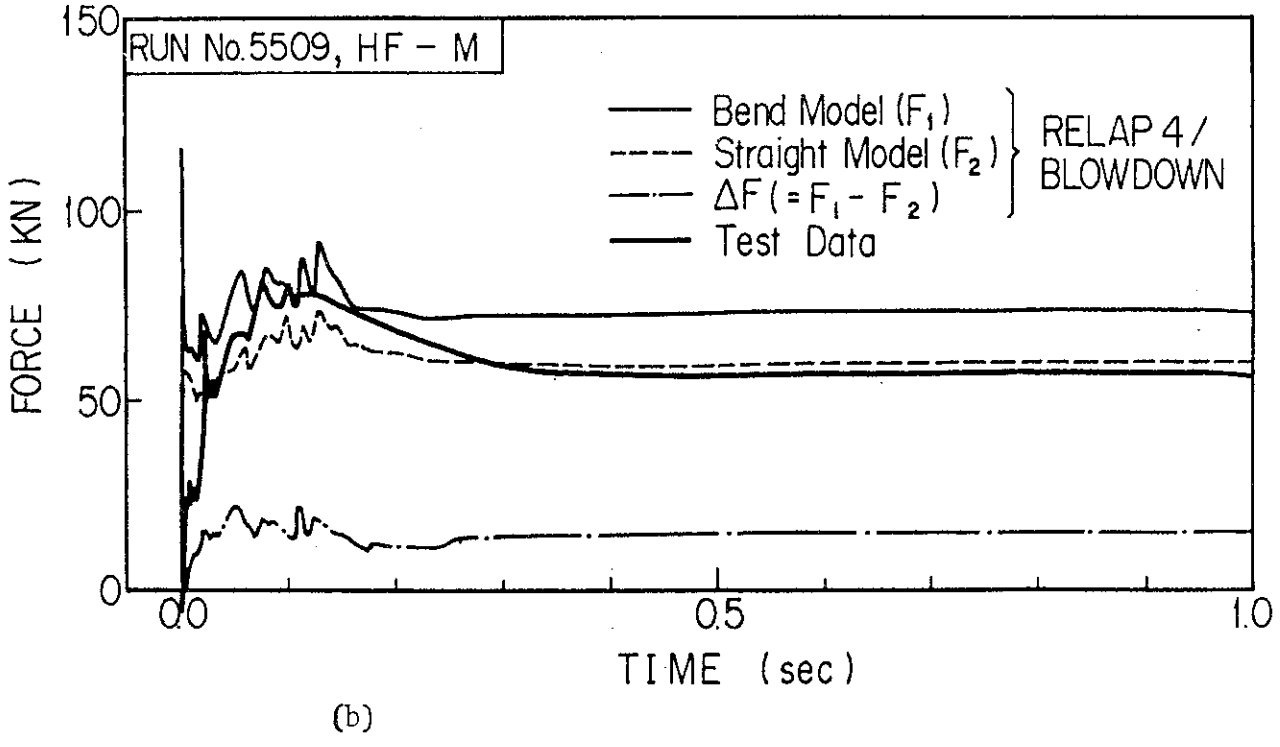

(b) HF-M Model

Fig.17 Comparison of Blowdown Force between RELAP4/BLOWDOWN Analysis and JAERI's Test

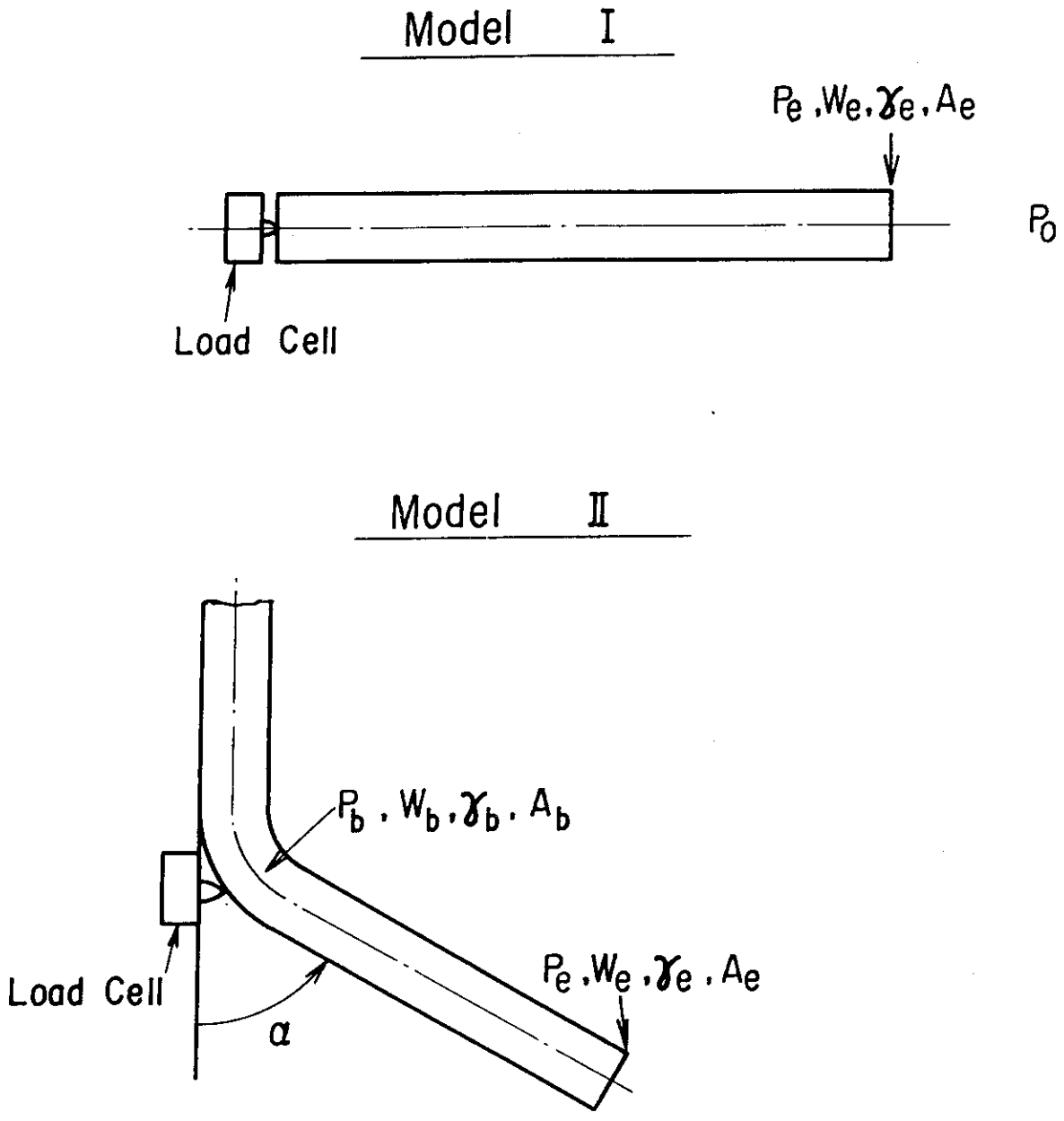

Fig.18 Schematic Figures of Straight Pipe Model and Bend Pipe Model
——— Model I and Model II correspond to Straight Pipe Model and Bend Pipe Model, respectively